A Thirst for Silver: Trade Shock, Taxation, and Local Unrest in Nineteenth-Century China*

Ting Chen† Jianan Li‡ Chong Pang§ Yuan Zi¶

June, 2026

Abstract

Under what conditions can globalization become a source of state fragility? We provide the first systematic evidence that rigid trade and taxation systems, together with the collapse in global silver production following the Spanish American wars of independence, fueled rising silver prices and social instability in early nineteenth-century Qing China. Using newly assembled county-level panel data and historical commercial routes, we show that regions farther from Canton—the empire's sole legal international port—experienced larger increases in silver prices and greater social unrest following the shock. Silver-denominated taxation was central to this relationship: because taxes were largely fixed in silver terms, rising silver prices sharply increased real tax burdens and fueled instability. Quantitatively, the silver shock reduced China's aggregate welfare by 1.16%, with fiscal rigidity accounting for most of the loss. Opening additional international ports would have mitigated the destabilizing effects of the shock, but only modestly. By contrast, fiscal reform would have been far more effective.

JEL classification: L52; F13; R38
Keywords: Trade Costs; Silver Shock; Fiscal Capacity; Social Unrest; Chinese Economy

*We are grateful to Rodrigo Adão, Johannes Boehm, Yiming Cao, Heng Chen, Carsten Eckel, Rui Estevens, Qin Jiang, Gabriel Kreindler, Zhan Lin, Ernest Liu, Chicheng Ma, Isabelle Mejean, Andreas Moxnes, Marcelo Olarreaga, Emanuel Ornelas, Ralph Ossa, Mathieu Parenti, Luigi Pascali, Nathan Sussman, Cedric Tille, Mathias Thonig, Erik H. Wang, Zi Wang, Anson Zhou, and participants from various seminars for their generous comments and suggestions. All remaining errors are our own.

†School of Business, Hong Kong Baptist University. Email: tingchen@hkbu.edu.hk.
‡School of Economics, Xiamen University. Email: jianan.li@xmu.edu.cn.
§Barcelona School of Economics and Universitat Pompeu Fabra. Email: chong.pang@bse.eu.
¶Geneva Graduate Institute and CEPR. Email: yuan.zi@graduateinstitute.ch.

1 Introduction

On an otherwise ordinary evening in 1838, Huang Juezhi, a mid-ranking imperial official, found himself unable to sleep. Restless, he rose and penned a memorial to the Emperor, writing:

"If, in the next few years, the price of silver continues to rise, how will expenditures be managed? How will taxes be collected? And if an unforeseen emergency arises, how could it be funded? Whenever I think of this, I toss and turn, unable to sleep."

What Huang described was not a new problem, but rather a predicament that had haunted the empire for decades. Between 1800 and 1850, the price of silver—a key currency for long-distance trade and state taxation, which China itself did not produce—more than doubled relative to copper coins, the currency of daily wages and consumption. This price surge ushered in the era famously known as the Daoguang Depression (1821–1850), a period of economic contraction marked by deflation, widespread poverty, and growing social unrest across the empire (von Glahn, 2018; Li, 2020; Lin, 2020). The mid-19th century thus marked a critical turning point in Chinese history: the Qing dynasty rapidly declined from "High Qing" prosperity into an "unprecedented great upheaval" (Wei Yuan, 1845) that defined China's entry into the modern era.

Under what conditions can global integration become a source of state fragility? We study this question through the silver crisis in early nineteenth-century China. Using modern quantitative trade models and novel historical data, we show that a global decline in silver production—triggered by the Spanish American wars of independence—fueled rising silver prices and social instability across the empire. Two rigid domestic institutions were central to this transmission: the Canton System, which restricted international trade to a single port of entry,[1] and a fiscal system that imposed largely fixed tax obligations denominated in silver.

With minimal domestic silver production, the Qing economy depended almost entirely on trade surpluses to sustain its monetary system—a vulnerability that became acute when global silver supplies contracted by nearly 50 percent after 1810 due to the Spanish American wars of independence. The Canton System funneled all legal international trade through a single port, so

[1] While the Canton System formally restricted *Western* maritime trade to Canton, other channels of silver inflow were negligible in scale. According to Lee (2009), Canton accounted for approximately 93% of China's net silver inflow during our sample period. We therefore refer to Canton as China's sole international port throughout the paper for conceptual simplicity.

the collapse of silver inflows propagated unevenly across the empire, leaving interior regions far from Canton most exposed to the shortage. The fiscal system then converted monetary scarcity into social pressure: most households used copper coins for daily transactions but owed taxes in silver at largely fixed amounts. As the price of silver rose, so did the real burden of taxation. In the end, although China was not particularly open to trade and silver played only a limited role in everyday transactions, domestic institutions transformed an external commodity shock into a monetary and fiscal crisis that strained Qing social stability and state capacity.

We establish this mechanism by bringing together newly digitized historical data, reduced-form evidence, and a quantitative spatial model. This approach yields three main contributions. Our first contribution is to digitize and georeference a large commercial network documented in *Shanggu Bianlan* ("A Convenient Handbook for Merchants"), a comprehensive merchant guidebook written in 1792 and widely used in Qing China. This source records 75 major trade routes as sequences of waypoints connecting commercial centers across the empire. We extract and geocode these waypoints, then construct the likely paths between them using least-cost path analysis that accounts for terrain, historical river systems, and the technological constraints of early nineteenth-century Chinese transportation. The resulting dataset provides, to our knowledge, the first systematic georeferenced representation of Qing China's commercial transportation network. Among others, we use this network to construct county-level measures of trade costs to Canton, which we show to be a strong predictor of local exposure to global silver supply shocks. Beyond the present study, this dataset offers a novel resource for research on historical trade, market integration, and economic geography in late imperial China.

Our second contribution is to provide the first systematic empirical evidence on how the early nineteenth-century silver shortage shaped social instability in Qing China. Using our newly constructed commercial network and a rich county panel covering 1,549 counties across China Proper (the 18 Han Chinese provinces) from 1801 to 1840, we establish three key findings. First, regions facing higher trade costs to Canton experienced significantly larger silver price increases when Mexican silver production declined. Second, regions with higher trade costs to Canton also experienced more conflict during periods of rising silver prices. Third, the rigid tax burden served as a key transmission channel: conditional on trade costs to Canton, regions with heavier tax burdens experienced even larger increases in conflict when silver prices rose. Our main results

are robust to instrumenting domestic silver prices with Mexican silver production or major mine disruption events during the Spanish American wars of independence, to the inclusion of various controls and alternative subsamples, and to alternative measures of trade costs to Canton. Falsification exercises confirm that trade costs to placebo ports, to political or economic centers, and the pre-Canton System period (before 1757) do not generate similar patterns. Finally, we present corroborating evidence that the effect is attenuated in regions with proximity to domestic silver mines, and that despite the government directing a larger share of relief to remote regions, total relief incidents, government expenditures, and revenues all contracted when silver prices rose—consistent with historical accounts of silver-scarcity–induced fiscal strain, further limiting state capacity to respond to the crisis.

Our final contribution is to develop and estimate a quantitative spatial model that incorporates international silver trade and taxation. Within each period, goods trade follows a standard Armington structure, and the rest of the world exchanges silver for goods produced in each Chinese region. Merchants face endogenous market penetration costs à la Arkolakis (2010) and endogenously choose the fraction of households to reach in each region, so that remote interior areas of Canton exhibit greater trade elasticities. Together with domestic trade, each region's overall trade surplus determines net silver inflows, which in turn governs the evolution of local silver prices and hence real tax burdens. We show analytically that the model can rationalize our three main empirical findings, with both the trade and taxation components being crucial for delivering the predictions. Quantitatively, the Spanish American silver supply shock reduced China's aggregate welfare by 1.16%, with silver-denominated taxation accounting for most of the loss. Contrary to the common narrative that greater trade openness would have benefited late imperial China, our counterfactual exercises suggest that opening additional international ports would have had limited effect in attenuating the welfare loss, whereas a simple fiscal reform—equalizing per-capita tax obligations across regions—emerges as a far more effective policy lever.

The findings of this paper thus speak to a general mechanism through which globalization can become a source of state fragility. External shocks become destabilizing not simply because they are large, or because economies are highly open, but because they pass through choke points that transmit and amplify their effects. Institutions are often overlooked as choke points, yet they can be among the most consequential. In our setting, the Canton System concentrated access to global

silver flows through a single port, while the fiscal system converted monetary scarcity into rising real tax burdens. This perspective speaks directly to contemporary debates over trade decoupling, sanctions, and supply-chain fragility, where consequences depend not only on exposure, but on where vulnerabilities lie.

Related Literature. Our paper contributes to the literature on trade and spatial economic outcomes in historical settings. A rich body of work has examined how transportation networks shape local economic and social outcomes: in historical context, Fogel (1964), Donaldson and Hornbeck (2016), and Hornbeck and Rotemberg (2024) study the impact of U.S. railroads on economic growth; Donaldson (2018) examines railroads in colonial India; Nagy (2023) traces the westward expansion of the United States; and Pascali (2017) evaluates the role of steamships in maritime trade and development. Others have studied the effects of political barriers—Redding and Sturm (2008) on the Iron Curtain in Germany, Ahlfeldt et al. (2015) on the Berlin Wall—and trade disruptions, such as Juhász (2018) on the Napoleonic blockade. Yet unlike the standard market access channels emphasized in these papers, we show that even in an economy with limited trade openness, foreign supply shocks can produce severe consequences when mediated by monetary systems and rigid domestic institutions. Conceptually, our framework is particularly informed by Boehm and Chaney (2024), who study the role of trade and technology through the diffusion of coinage in the ancient world. Although the questions differ, both papers highlight how monetary circulation and trade geography interact in pre-modern economies.

Our paper also speaks to the literature on the real effects of money in historical settings, recently surveyed by Brzezinski et al. (2024b). In particular, Palma (2022) and Brzezinski et al. (2024a) exploit exogenous disruptions to precious metals supply from the Americas—through colonial production cycles and maritime disasters, respectively—to show that monetary contractions generated persistent real output losses in early modern Europe. Our identification similarly exploits exogenous changes in silver supply from the Americas. While these studies estimate aggregate effects at the national level, we trace how a global monetary contraction propagates spatially within a large economy, and find that its distributional consequences are themselves a quantitatively important driver of aggregate welfare losses and social instability. More broadly, our fiscal transmission channel resonates with the debt deflation mechanism of Fisher (1933): just as falling prices inflate the real burden of nominal private debt, rising silver prices mechanically

raised the real cost of fixed, silver-denominated tax obligations.

Our study also contributes to the long-standing debate over the origins of turmoil and recession in nineteenth-century China. Traditional historiography attributes this crisis to climate shocks (Cao et al., 2012; Li, 2015), Malthusian pressures (Jones and Kuhn, 1978; Huang, 1990), or dynastic cycles (von Glahn, 2018). We depart from this literature by focusing on trade-induced monetary disruption—specifically, the silver shortage triggered by the Spanish American wars of independence, which Lin (2020) suggests precipitated a severe economic depression across China (Ma, 2012; Wang, 1997). While this channel has attracted growing attention, the existing literature remains descriptive and historical in nature; the closest precedent is Bai and Kung (2018), who document a time-series correlation between rising silver prices and declining living standards. We go substantially further. Using a rich dataset we assembled alongside a reconstructed historical commercial network, we establish the causal link between the collapse in silver inflows and social unrest. We then develop a theoretical framework that articulates the mechanism and quantifies the aggregate welfare cost by combining data with the model. Our work thus provides the empirical and theoretical foundation for Lin (2020)'s influential conjecture.

Finally, our paper speaks to the literature on trade and conflict (Martin et al., 2008; Vicard, 2012; Berman et al., 2017; Dell et al., 2019; Cao and Chen, 2022; Couttenier et al., 2024). Our setting again departs from the standard channels: we add to the literature by showing that foreign supply shocks can fuel domestic conflict not only through direct trade exposure, but also through their interaction with rigid institutional structures. To our knowledge, this is among the first studies to bring both credible causal identification and structural quantification to bear, in both the trade–conflict literature and the Chinese economic history studies.

The remainder of the paper is organized as follows. Section 2 reviews the historical background and describes the data. Section 3 presents the empirical results. Section 4.1 introduces the model and derives the comparative statics. Section 5 describes the model's parameterization and presents the quantitative results. Section 6 concludes.

2 Historical Background and Data

This section provides historical context for our analysis and introduces the key datasets. We refer readers to the Data Appendix A for full variable definitions and sources.

2.1 The Canton System and Trade Costs

The Canton System was a Qing policy that confined all Western maritime trade to a single port—Canton—under a tightly regulated institutional framework.[2] This arrangement effectively centralized maritime silver inflows at one entry point, making Canton the dominant conduit for silver entering the empire. The policy built on the Qing state's longstanding suspicion of maritime activity—shaped by early coastal conflict and intermittent sea bans—but it emerged in its institutionalized form in the mid-eighteenth century. After a brief period in which foreign trade was permitted at multiple ports, Emperor Qianlong restricted all Western maritime commerce to Canton in 1757, following repeated conflicts with British traders at Ningbo, thereby formally establishing the Canton System (Van Dyke, 2005). This regime remained in place until the Treaty of Nanking in 1842.

Under the system, all foreign trade had to be conducted through the *Cohong*, a guild of licensed intermediaries (Wakeman, 1978). Foreign merchants were confined to a small district outside Canton's city walls during the trading season and were prohibited from direct contact with Chinese civilians and local officials (Fang et al., 1996–2014). As a result, silver payments for Chinese exports entered the empire almost entirely through Canton. Other channels of silver inflow existed but were quantitatively limited: trade with Japan had declined substantially by the eighteenth century, overland Central Asian routes remained modest in scale, and coastal smuggling constituted only a small fraction of total inflows during the period (Morse, 2007; Lee, 2009). According to Lee (2009), Canton accounted for approximately 93% of China's net silver inflow during our sample period (1801–1840).

Because silver served as the medium of exchange, its regional distribution reflected underlying trade balances: silver flowed into regions running trade surpluses and out of those running

[2]Canton was a coastal prefecture in southern Qing China, adjacent to Hong Kong, and corresponds to present-day Guangzhou.

deficits (Feuerwerker, 1980). Since foreign trade was concentrated in Canton, regions farther from Canton faced higher effective trade costs, participated less in export-oriented commerce, and consequently received fewer silver inflows. In the absence of an integrated financial system capable of redistributing these monetary imbalances,[3] distance from Canton generated persistent spatial variation in silver availability—a disparity that became especially consequential during periods of aggregate monetary contraction.

Trade Cost to Canton. To measure each county's exposure to silver supply shocks, we construct trade costs to Canton using GIS methods and detailed historical sources. Our primary data source is the *Shanggu Bianlan* ("A Convenient Handbook for Merchants"), a Qing-era commercial guide documenting 75 major trade routes across China Proper. Unlike sources that record only origin–destination pairs, this guide reports detailed waypoint sequences—the intermediate stops along each route—which provide rich information about the actual paths merchants traveled (see Figure A1). We digitize and georeference these sequences, yielding 630 unique route segments that form the backbone of our historical trade network.

Because the *Shanggu Bianlan* records waypoints rather than exact paths, we use least-cost path analysis to model routes between consecutive waypoints. The geospatial model combines high-resolution elevation data with historical waterway networks to estimate travel routes that minimize time and cost, reflecting the technological constraints of pre-modern Chinese commerce. Water transport serves as the baseline mode, while overland travel costs rise steeply with terrain slope following an adapted Tobler hiking function. As shown in Figure 1-(a), the resulting network closely matches historical patterns: it favors waterways and largely avoids mountainous regions. Full details on cost surface construction and parameter calibration are provided in the Data Appendix (Section A.1).

We validate the geospatial model by comparing estimated travel distances with directly recorded distances in the *Shanggu Bianlan* for waypoint connections where such records exist. As shown in Figure B4, estimated distances closely track historical records, yielding a coefficient of 0.97

[3]Remittance banks (*piaohao*) remained geographically limited and played only a minor role during our sample period. According to Du et al. (2024), *piaohao* branches operated in only about 10% of prefectures in South China in the 1850s, implying even more limited coverage in 1801–1840. Moreover, *piaohao* primarily served merchants and officials rather than ordinary households.

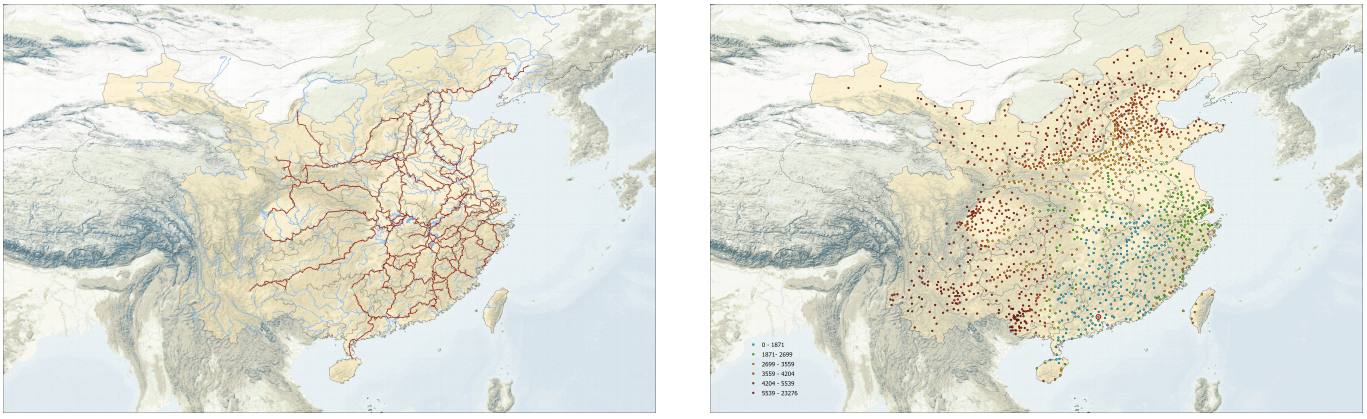

(a) Estimated Trade Network (b) Travel Cost to Canton

Notes: Panel (a) shows the spatial distribution of the estimated trade network, and Panel (b) reports the distribution of travel costs to Canton. In Panel (b), the unit is the cost of traveling 1 km along natural waterways within the network.

Figure 1: Estimated Trade Network and Travel Cost to Canton

(R^2 = 0.82) in a simple OLS regression, while straight-line distance performs substantially worse, particularly for longer routes where it severely understates actual travel distance.

For counties not directly located on the trade network, total trade costs are then constructed as the sum of off-network travel to the nearest network point and on-network travel from that point to Canton along the least-cost path. This reflects the historical practice that merchants from remote areas would first connect to established routes before proceeding to major commercial centers. Following Bai et al. (2025), off-network travel is assigned a cost multiplier of 6 to capture poorer road conditions and security risks.[4] Figure 1-(b) shows the resulting trade cost estimates, which display substantial geographic variation driven by both distance and terrain: counties in the North China Plain benefit from low costs due to favorable terrain and access to the Grand Canal, while some mountainous southwestern counties face much higher costs even when geographically closer to Canton.

2.2 The Qing Tax System

The Qing fiscal system was characterized by rigid and highly persistent land taxation. In 1712, the Kangxi Emperor issued the landmark decree that "the population born in this prosperous era shall never be subject to additional taxation" (*shengshi zisheng rending, yong bu jiafu*), effec-

[4]Robustness checks consider alternative multipliers ranging from 1 to 10.

tively freezing the poll-tax base at its 1711 level (Ho, 1959). At the time, land and poll taxes were levied separately, broadly following Ming Dynasty institutions. Rapid population growth during the eighteenth century, however, rendered the poll tax increasingly difficult to administer and disconnected tax liabilities from actual demographic conditions. In response, the Yongzheng Emperor (reign 1723–1735) implemented reforms that merged poll taxes into the land tax (*tan ding ru mu*), effectively transforming the system into a land-based fiscal regime (Guo, 2022). Although tax obligations continued to be described as "land-and-poll" taxes (*diding*), they had by then become effectively fixed levies assessed per unit of registered land. Crucially, these obligations were denominated in silver and remained highly inflexible over time, with assessments largely tied to historical quotas rather than contemporaneous economic conditions.

Overall, the Qing fiscal system relied heavily on land taxation and remained remarkably stable over time. The land-and-poll tax accounted for approximately 70% of central government revenue (Wang, 1973), and the basic structure of the system remained largely unchanged throughout the early nineteenth century, persisting until the fiscal reforms following the Taiping Rebellion in the 1950s. Importantly, per-*mu* tax burdens varied substantially across regions, but these differences were largely predetermined by historical legacies rather than contemporaneous economic conditions.[5]

On the expenditure side, Qing fiscal priorities were highly hierarchical and heavily skewed toward maintaining the state apparatus. Military salaries for Manchu and Han troops absorbed roughly 60% of government spending, followed by another 30% devoted to official salaries and administrative allowances. Only a small residual financed public goods such as courier stations, river conservancy, and grain transport infrastructure, while disaster relief and other transfers constituted a negligible share (Myers and Wang, 2002). From the perspective of the eighteen Han provinces that bore most of the tax burden, the system was therefore primarily extractive.

Tax Data. We measure historical tax burdens using county-level land-and-poll tax (*diding*) data compiled by Guo (2022) from the *Jinshenlu*, which record total collections denominated in silver

[5]For example, commercially productive regions such as Jiangnan had borne heavy fiscal obligations since the Ming dynasty, while frontier areas often received preferential assessments to encourage settlement (Wang, 1973; He, 2008). A Chinese *mu* is a traditional unit of land measurement, roughly 1/15th of a hectare.

taels.[6] We use the 1760 cross-section—the closest available year prior to our sample period—to minimize endogeneity concerns. To facilitate comparison across counties of different sizes, we construct three measures of land-tax burdens by normalizing total collections by potential agricultural income (from GAEZ data), cultivated farmland area, and population, respectively.

2.3 Silver in the Qing Economy

The Qing dynasty operated under a bimetallic monetary system in which copper coins and silver performed distinct economic functions.[7] Copper coins, minted by central and provincial authorities, were used primarily for local retail transactions, with coin circulation remaining highly regionalized (Peng, 2020). Silver, by contrast, served as the principal medium for tax payments, official salaries, large-scale commerce, and interregional exchange (Wang, 1981; Peng, 2020).[8] Unlike copper coinage, which was regulated through official minting, silver circulated freely in the form of both domestic *sycee* ingots and foreign coins (King, 1965).[9] In the absence of an integrated financial system, regional silver availability depended heavily on trade flows and access to long-distance commerce.

China possessed negligible domestic silver resources, accounting for only approximately 0.01% of world output between 1493 and 1927 (Vilar, 1991). China's money supply therefore depended overwhelmingly on imported silver, most of which ultimately originated from Latin America; an estimated 40% of global silver production flowed into China between 1500 and 1800 (Flynn and Giráldez, 2022). [10] Contract records from Quanzhou, a major port city in Fujian province, illustrate the growing dominance of foreign silver (Figure B2). Around 1710, nearly all contracts

[6] The *Jinshenlu* is a comprehensive Qing administrative registry updated at regular intervals, providing systematic and longitudinal records of tax collections across all administrative jurisdictions in the Qing empire.

[7] Although Chinese governments experimented with paper money as early as the thirteenth century, these experiments often resulted in severe inflation (Ma, 2012). Concerns over monetary instability, together with sustained silver inflows through foreign trade, contributed to the emergence of a copper-silver dual currency system from the late Ming dynasty onward (von Glahn, 2023). The Qing government itself issued no paper currency between 1661 and 1853 (Peng, 2020).

[8] The use of silver for tax payments dated to the Ming dynasty's "Single Whip Reform," which consolidated various in-kind levies and labor obligations into a single payment denominated in silver. Because most ordinary households earned income in copper-denominated local markets, they needed to convert copper earnings or agricultural output into silver to meet tax obligations.

[9] Market participants developed sophisticated methods for assessing silver weight and purity (King, 1965).

[10] The foreign origin of circulating silver, together with the Qing state's limited involvement in foreign trade before the mid-nineteenth century, may also help explain why the state never attempted to monopolize silver circulation.

specified payment in domestic *sycee* silver, whereas by 1800 approximately 80% were denominated in foreign silver coins, with Mexican silver dollars accounting for nearly 60% of transaction values.

This deep integration with global silver flows meant that China's monetary conditions were tightly linked to developments in overseas producing regions. Table B1 documents this connection. Net silver inflows to China were negatively associated with domestic silver price growth: a one-million-tael increase in inflows corresponded to a 0.14 percentage point decline, equivalent to roughly 30% of the pre-shock average growth rate (columns 1–2). Mexican silver production was also positively associated with China's net inflows: a 10% increase corresponded to an additional 0.10–0.16 million taels flowing into China (columns 3–4). Together, these results indicate that fluctuations in Latin American silver production were transmitted to China's domestic silver prices.

Data on Mexican Silver Production. Our empirical analysis exploits exogenous variation in Mexican silver production to identify the effects of silver scarcity and rising silver prices on Chinese economy. Annual data on Mexican silver coin production come from Borah (1949), who compiled comprehensive records from colonial Spanish and later Mexican mint archives.[11] As shown in Figure 2, Mexico dominated global silver production before 1810, accounting for approximately two-thirds of world output in the early nineteenth century.

Data on Silver Prices. We employ two sources of silver price data. Our primary measure is the nationwide silver–copper exchange rate series constructed by Lin (2020), drawn from the commercial ledger of a large chain store in Zhili Province during our sample period (1801–1840).[12] To study regional heterogeneity, we supplement this series with a provincial panel compiled by Hu (2021), covering 279 province-year observations. Because the provincial data contain substantial missing values, we use them only in specifications that require cross-regional variation in silver prices.

[11] For years after 1821, Borah (1949) reports only the combined production of silver and gold coins; Figure 2 plots the raw series. For the empirical analysis, we adjust the post-1821 series using the gold-silver production ratio observed during the pre-independence period (1801–1821). Further details are provided in Appendix A.

[12] During this period, goods prices and wages were relatively stable in terms of copper coins, as illustrated by the Beijing series in Figure B3, while the silver–copper exchange rate increased substantially over time. Conceptually, we therefore use the local price of silver as an inverse measure of the local price index.

Notes: This figure plots Mexico's annual silver coin production (orange line) and world silver production (gray bars) from 1720 to 1870. The vertical line marks the onset of the Spanish American wars of independence (1808–1826). Mexico's annual silver coin production data are from Borah (1949), as described in the Data Appendix. World silver production data are from Merrill and Staff of the Common Metals Division (1930), which reports multi-year aggregates that we convert to annual averages for plotting.

Figure 2: World and Mexico Silver Production

2.4 The Spanish American Wars of Independence

The Spanish American wars of independence triggered a major contraction in global silver supply. Beginning around 1808 after Napoleon's invasion of Spain, the conflicts spread across Latin America and severely disrupted production in the world's principal mining regions. At the time, Spanish America, especially Mexico, accounted for more than two-thirds of global silver production. As shown in Figure 2, Mexican silver output fell by more than half within a decade after 1810, while global production remained depressed until the 1870s.

For China—the world's largest silver-absorbing economy—the consequences were substantial. China lost an estimated 16.4% of its silver stock between 1808 and 1856 (Lin, 2020), contributing to a sustained increase in domestic silver prices. Between 1810 and 1840, silver prices rose at an annual rate of 1.25%, nearly triple the 0.42% rate observed during 1721–1810 (Figure 3). Over the first half of the nineteenth century, the silver–copper exchange rate more than doubled. Contemporary accounts also noted substantial regional variation in silver prices, with inland regions and counties distant from trade opportunities experiencing particularly sharp increases (Lin, 2020).

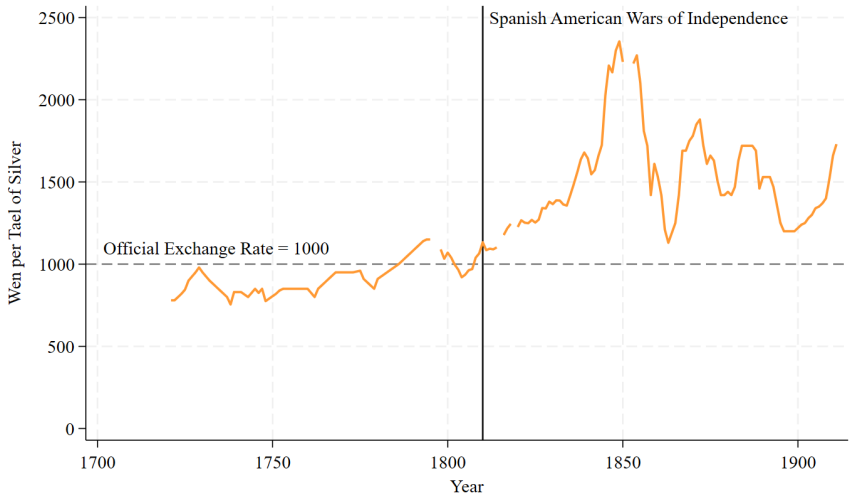

Notes: This figure plots the annual silver price in China from 1700 to 1911, measured as the number of copper cash (wen) per tael of silver. The horizontal dashed line indicates the official exchange rate of 1,000 wen per tael. The vertical line marks the onset of the Spanish American wars of independence (1808–1826), which disrupted global silver flows. Data are from Lin (2020).

Figure 3: Silver Price Fluctuations

Data on Unrest. To measure social instability, we construct an annual county-level panel of conflict frequency from the *Qingshilu* (Veritable Records of the Qing Dynasty). The *Qingshilu* constitutes the official chronicle of the Qing court, compiled from imperial diaries, memorials, and edicts, and provides systematic coverage of local disturbances reported to the central government (Kuhn, 1990). The recorded incidents include banditry and localized violence (*fei ni*), tax resistance (*kang zu kang shui*), and unrest surrounding famine relief distribution (*qiang mi nao zhen*). Unlike the large-scale uprisings commonly studied in the modern conflict literature (Fearon and Laitin, 2003), most incidents in our data represent small-scale, localized disturbances involving dozens or at most hundreds of participants and typically contained within county boundaries. Because the distinction between categories was often blurred in practice, we focus on the aggregate frequency of unrest as a measure of general social instability.[13] Figure B1 in the Appendix plots annual unrest frequency and shows a marked increase during our sample period, with recorded incidents in the decade immediately before the Opium War nearly doubling relative to the first decade of the nineteenth century.

[13] Appendix A.4 provides additional discussion of the classification and reporting of local unrest in *Qingshilu*.

2.5 Additional National and Regional Characteristics

Our empirical analysis controls for a broad set of political, social, geographic, and economic characteristics that may shape local exposure and responses to silver supply shocks. To account for differential vulnerability to time-varying monetary shocks, we interact these historical and geographic characteristics with annual measures of Mexican silver production or domestic silver price growth, depending on the specification. Specifically, we construct controls using the following historical and geospatial data sources:

Political classifications—whether a county was designated as a transportation hub (*Chong*), administratively complex (*Fan*), fiscally distressed (*Pi*), or difficult to govern (*Nan*)—are drawn from Liu (1993). These designations were established in 1728 and therefore predate our sample period. *Social norms* are proxied by the number of pre-1750 genealogies from the *Comprehensive Catalogue of Chinese Genealogies*. *Geographic variables* include longitude, latitude, elevation, county area (proxied using Thiessen polygons constructed from 1820 county centroids in CHGIS), and agricultural suitability from Galor and Özak (2016). *Domestic currency sources* are measured using distances to the nearest silver mines based on location information from Wei (1983).

We also control separately for the annual incidence of five natural disasters—droughts, floods, frosts, hail, and snow—using data from the *Comprehensive Gazetteer of Chinese Meteorological Disasters* (Zhang, 2013). In robustness checks, we additionally account for major export commodities (ceramics, silk, and tea), opium trade exposure (Richards, 2002), proximity to the Grand Canal (Cao and Chen, 2022), and exposure to the White Lotus Rebellion (Dai, 2019). Section A.6 of the Data Appendix provides detailed variable definitions and sources. Unless otherwise noted, all control variables are log-transformed. Table A1 summarizes variable definitions, sources, and summary statistics.

3 Empirical Results

We organize our empirical analysis around three findings: how trade costs to Canton shaped local silver price responses to fluctuations in Mexican silver production, how price increases translated

Table 1: Provincial Silver Price Responses to Mexican Shock

	$\Delta Silver_{pt}$		
	(1)	(2)	(3)
$TradeCanton_p \times MexicoSilver_t$	-0.0774*	-0.1396**	-0.1427**
	(0.0434)	(0.0642)	(0.0650)
Baseline Controls	No	No	Yes
$Distance_p \times MexicoSilver_t$	No	Yes	Yes
Province FE, Year FE	Yes	Yes	Yes
Observations	185	185	185
R-squared	0.413	0.421	0.445

Notes: The dependent variable is the log change in provincial silver prices relative to copper, calculated based on Hu (2021). The data sample is an unbalanced panel and includes 18 Han-inhabited provinces of China Proper, covering the years 1801 to 1840. $TradeCanton_p$ represents the average of the log travel cost from each province to Canton; $MexicoSilver_t$ represents the log of Mexico's silver production, calculated based on Borah (1949); $Distance_p$ represents the average of the log straight line distance to Canton. Coefficients are estimated using OLS, with robust standard errors reported in parentheses. *** $p < 0.01$, ** $p < 0.05$, * $p < 0.1$.

into higher conflict incidence, and how heavier tax burdens amplified the effect. A supplementary subsection further provides suggestive evidence on the government's constrained capacity to respond.

3.1 Distance to Canton and Silver Price Changes

As a first step, we establish how trade costs to Canton shaped local silver price responses to Mexican production shocks. Table 1 reports results from regressing provincial silver price changes on the interaction between trade costs to Canton and Mexican silver production.

Column (1) includes province and year fixed effects. The negative coefficient on the interaction term indicates that provinces with higher trade costs to Canton experienced larger silver price increases, reflecting more severe local silver scarcity, when Mexican production declined. Column (2) adds an interaction with straight-line distance to Canton to control for the possibility that trade costs simply proxy for other geographic factors. The trade cost coefficient becomes larger and more precisely estimated, confirming that travel costs through trade networks, rather than geographic proximity only, drives the heterogeneous price response. Column (3) adds controls for county-level natural disaster frequencies, and the result remains robust. The preferred specification (3) implies that a one-standard-deviation increase in trade costs to Canton (0.70) amplified the local silver price's negative response to Mexican supply shocks by approximately 10

Table 2: Conflict Incidence and Trade Costs to Canton

	$Conflicts_{it}$		
	(1)	(2)	(3)
$TradeCanton_i \times \Delta Silver_t$	2.5129	4.9070**	10.3170***
	(2.0418)	(2.2490)	(3.6192)
Baseline Controls	No	No	Yes
$Distance_i \times \Delta Silver_t$	No	Yes	Yes
County FE, Year FE	Yes	Yes	Yes
Observations	36180	36180	36180
Pseudo R-squared	0.359	0.359	0.361

Notes: The dependent variable is the number of conflicts for a given county and year. The sample covers 1,515 counties within the 18 Han-inhabited provinces of China Proper from 1801 to 1840. $TradeCanton_i$ represents the log of the travel cost from each county to Canton; $\Delta Silver_t$ represents the log change in silver prices relative to copper, calculated based on Lin (2020). $Distance_i$ represents the log of the straight line distance to Canton. Coefficients are estimated using a pseudo-Poisson model, with standard errors clustered at the prefecture level reported in parentheses. Significance levels: *** $p < 0.01$, ** $p < 0.05$, * $p < 0.1$.

percentage points.

3.2 Linking Silver Price Changes to Conflict Incidence

We now turn to our main results, examining how rising silver prices contributed to local social instability and how this effect varied with counties' trade costs to Canton. Table 2 presents county-level estimates showing that regions with higher trade costs to Canton experienced more conflict during periods of rising silver prices. The dependent variable is the count of conflicts in each county-year, and estimates are obtained using Poisson pseudo-maximum-likelihood (PPML). The key regressor is the interaction between trade costs to Canton and the annual log change in silver prices. Combined with the evidence in Table 1, this interaction captures heterogeneous local exposure to aggregate movements in silver prices.

Column (1) reports a parsimonious specification with only fixed effects. The coefficient on the interaction term is positive but imprecisely estimated. Column (2) adds an interaction between straight-line distance and silver price changes, absorbing variation due to simple geographic remoteness; the interaction term becomes statistically significant at the 5% level. Column (3) introduces the full set of baseline controls: county-level natural disaster frequency and interactions between silver price changes and geographic characteristics (longitude, latitude, elevation, area), agricultural suitability, social norms, and political-military classifications from 1728, as detailed

Table 3: Falsification Tests

	$Conflicts_{it}$			
	Placebo Ports	Beijing 1801-1840	Nanjing	Placebo Period 1721-1757
	(1)	(2)	(3)	(4)
$TradeCost_i \times \Delta Silver_t$	-4.5283	-0.3272	-3.4014	
	(5.0719)	(3.9141)	(3.5295)	
$TradeCanton_i \times \Delta Silver_t$	10.6928**	9.6620**	11.6374***	-1.1313
	(5.0719)	(4.2041)	(4.1679)	(1.8079)
Baseline FEs and Controls	Yes	Yes	Yes	Yes
Observations	36180	36180	36180	27540
Pseudo R-squared	0.362	0.361	0.361	0.300

Notes: This table replicates the regression from Table 2, column (3), with placebo tests. In columns (1)–(3), the log trade costs to Canton are replaced with alternative measures. Column (1) uses the log of the average travel cost to three other port cities opened for a period after the return of Taiwan (Zhangzhou, Songjiang, and Ningbo; opened 1684–1757). Columns (2) and (3) use log trade costs to political centers, Beijing and Nanjing, respectively. These regressions also control for the interaction between log trade costs to Canton and log silver price changes. Column (4) conducts a placebo test using the pre-sample period (1722–1757). Coefficients are estimated using a pseudo-Poisson model, with standard errors clustered at the prefecture level reported in parentheses. Significance levels: *** $p < 0.01$, ** $p < 0.05$, * $p < 0.1$.

in Section 2.5. The coefficient rises substantially to 10.32 (significant at the 1% level), suggesting that omitted factors likely attenuate rather than exaggerate the baseline effect. This pattern is intuitive. Regions with strong social norms of connectivity may have had greater access to informal risk-sharing networks (Kung and Ma, 2014), while regions with greater political-military importance may have faced tighter social control by local elites; both channels would dampen conflict responses to silver shortages. The estimated effect is economically meaningful. In our preferred specification (column 3), a one–standard-deviation increase in silver price growth (0.03) implies that a county at the 75th percentile of trade costs to Canton experiences about 24% more conflicts than a county at the 25th percentile.[14]

Falsification Tests. A key concern about our baseline findings is whether the results actually reflect the role played by the Canton system. For instance, counties far from Canton would simply be remote frontier regions, which may differ systematically in conflict propensity or state capacity. We address this through several placebo exercises. If our results reflect the specific role of Canton rather than spurious correlations with distance to coastal or political centers, then trade costs to alternative locations should not predict conflict in the same manner.

[14]The difference in $TradeCanton_i$ between counties at the 75th and 25th percentiles is 0.685. The implied effect is computed as $10.317 \times 0.03 \times 0.685 \approx 0.212$, which translates into a percentage change of $(\exp(0.212) - 1) \times 100 \approx 24\%$.

Table 4: Results from Instrumental Variables

	$Conflicts_{it}$			
	(1)	(2)	(3)	(4)
	First Stage			
$TradeCanton_i \times MexicoSilver_t$	-0.0042***	-0.0042***		
	(0.0000)	(0.0000)		
$TradeCanton_i \times I(1810 \geq t \geq 1821)$			0.0267***	0.0268***
			(0.0019)	(0.0019)
$TradeCanton_i \times I(t > 1821)$			0.0219***	0.0220***
			(0.0013)	(0.0013)
	Second Stage			
$TradeCanton_i \times \Delta Silver_t$	13.0938**	12.1541**	2.3631***	2.1602**
	(5.6266)	(5.7632)	(0.8912)	(0.9011)
Baseline FEs and Controls	Yes	Yes	Yes	Yes
$ExportGoods_i \times MexicoSilver_t$	No	Yes	No	No
$ExportGoods_i \times I(1821 \geq t \geq 1810)$	No	No	No	Yes
$ExportGoods_i \times I(t > 1821)$	No	No	No	Yes
Observations	54540	54540	54540	54540
Kleibergen-Paap Wald rk F Statistics	174345	211774	14153	13244

Notes: This table revisits the estimation in Table 2, column (3) using an IV specification. Columns (1)–(2) use the interaction between $TradeCanton_i$ and the log of Mexico's silver production as the instrument, while columns (3)–(4) use the interaction between $TradeCanton_i$ and wartime dummies. Column (2) also controls the interactions between three export indicators (silk, tea, ceramics) and the log of Mexico's silver output; column (4) includes similar controls interacted with wartime dummies. Standard errors clustered at the prefecture level are in parentheses. *** $p < 0.01$, ** $p < 0.05$, * $p < 0.1$.

Table 3 presents the results. Columns (1) –(3) replace the interaction term with placebo trade costs to other historically significant locations, while controlling for trade costs to Canton interacted with silver price changes. Column (1) uses the average travel cost to three ports—Zhangzhou, Songjiang, and Ningbo—that were opened for foreign trade before the Canton system was established in 1757. The placebo coefficient is statistically insignificant, while the Canton interaction remains significant. Columns (2) and (3) use trade costs to political centers—Beijing and Nanjing, respectively.[15] Neither coefficient is significant, and the Canton effect, if anything, strengthens. Column (4) conducts a temporal placebo test using the pre-sample period 1722–1757, before the Canton System was introduced. The coefficient on the Canton interaction turns negative and insignificant, suggesting that our mechanism operated specifically during the Canton monopoly era.

[15]To be consistent with the specification in Table 2, we also control for straight-line distance to placebo locations interacted with $\Delta Silver_t$; excluding this control does not meaningfully affect our results.

IV Results. A potential concern with our main findings is that they may capture concurrent shocks that increased social unrest in a spatially uneven manner, rather than the external shock itself. For instance, the White Lotus Rebellion (1796–1804) preceded our sample period, and its aftermath—including displaced populations, weakened local governance, and residual banditry—may have differentially affected remote regions. More generally, any unobserved shock correlated with both trade costs to Canton and conflict propensity could confound our estimates.

To address this, Table 4 presents two-stage least squares (2SLS) estimates exploiting two sources of exogenous variation in China's silver supply. Columns (1)–(2) instrument the interaction between trade costs to Canton and Chinese silver prices using the interaction between trade costs to Canton and the log of Mexico's annual silver production. The identifying assumption is that Mexican silver output—determined largely by wartime disruptions and local mining conditions in Spanish America—affected Chinese conflict only through its impact on silver availability. The first stage is strong: a decline in Mexican production significantly increased the silver price exposure of remote counties. The second-stage coefficient remains positive and significant, with a magnitude similar to the baseline estimates.

Columns (3)–(4) of Table 4 employ an alternative instrument based on wartime events. We interact trade costs to Canton with indicator variables for the two phases of the Spanish American independence wars: 1810–1821 and post-1821. The first phase corresponds to the Mexican War of Independence, which began with the *Grito de Dolores* in 1810 and severely disrupted production from Mexico's silver mines. The second phase captures the subsequent disruption of Andean silver production as Peru declared independence in 1821 and Upper Peru (Bolivia) followed in 1825. Together, Mexico, Peru, and Bolivia accounted for approximately 85 percent of world silver production during this period (Borah, 1949). The first-stage coefficients confirm that remote counties experienced larger silver price increases during both wartime phases. The second-stage estimates remain positive and significant, though smaller in magnitude than those using Mexican silver production, consistent with the coarser variation captured by the wartime indicators.

In columns (1) and (3), we retain the same baseline controls and fixed effects as in Table 2, column (3), except that all controls interacted with silver price growth are instead interacted with the corresponding instruments. Columns (2) and (4) additionally control for interactions between the respective instruments and export commodity indicators (silk, tea, and ceramics), addressing the

possibility that the independence movements affected China not only through silver scarcity, but also through reduced external demand for Chinese exports. The results remain robust, suggesting that the monetary effects of silver scarcity drove the observed conflict patterns.

Additional Robustness Checks. We conduct a series of additional robustness checks reported in the Appendix B.

Table B2 examines the sensitivity of our main results to alternative controls and sample restrictions. Column (1) adds the interaction between an indicator for counties traversed by the Grand Canal and a post-1826 dummy, controlling for the differential impact of Grand Canal disruptions on canal-adjacent regions (Cao and Chen, 2022). Column (2) includes province-year fixed effects to absorb province-specific time-varying trends. Columns (3) and (4) control for interactions between silver price changes and, respectively, three export commodity indicators (silk, tea, and ceramics) and trade route intensity (total road network length in the county), addressing concerns that commercially advanced regions may have been differentially affected. Column (5) controls for the interaction between opium imports and trade costs to Canton. We note that the opium trade may itself be partly endogenous to silver prices, as silver scarcity incentivized the substitution of opium for silver in trade settlement; the stability of our coefficient nonetheless suggests that our main results are not driven by opium-related confounds. Columns (6) and (7) exclude provinces affected by the White Lotus Rebellion and Guangdong Province (where Canton is located), respectively. Across all specifications, the coefficient of interest on $TradeCanton_i \times \Delta Silver_t$ remains positive and statistically significant.

Table B3 and Figure B5 examine the sensitivity of our results to alternative constructions of trade costs to Canton. Table B3 replicates the baseline analysis using a simplified measure of travel costs based on straight-line distances between waypoints in the commercial road network and for off-path travel, rather than terrain-adjusted routes. The estimated effects remain qualitatively similar, though somewhat attenuated, consistent with increased measurement error. Figure B5 further re-estimates the baseline specification using off-route cost ratios ranging from 1 to 10, where the ratio represents the multiplicative penalty for travel outside the main trade network. Across all specifications, the coefficient on $TradeCanton_i \times \Delta Silver_t$ remains positive and statistically significant. Together, these exercises suggest that our findings are not driven by the

specific construction of the travel cost measure.

Finally, Table B4 provides indirect support for the silver scarcity mechanism by examining whether proximity to domestic silver mines mitigated the estimated effects. We split the sample based on counties' proximity to domestic silver sources. The interaction between trade costs to Canton and silver price growth is statistically significant only for counties located far from domestic silver mines (columns 1 and 3). For counties with better access to domestic silver, the estimated effects are substantially smaller and statistically insignificant (columns 2 and 4). This pattern suggests that domestic silver supply partially substituted for imported silver, mitigating the local economic stress associated with silver scarcity.

3.3 Tax Burden Matters

Because taxes were denominated in silver, rising silver prices mechanically increased real tax burdens for households operating in largely copper-based local economies. In an agricultural economy with limited surplus, this increase could substantially intensify local economic distress. Regions facing heavier tax burdens should therefore experience larger increases in conflict during periods of silver scarcity. Table 5 tests this mechanism by introducing a triple interaction between trade costs to Canton, silver price changes, and local tax burden.

We employ three alternative measures of tax burden, each capturing a different dimension of fiscal pressure. Column (1) uses the prefecture-level tax rate, defined as total tax revenue in 1760 divided by potential agricultural income. Column (2) uses county-level taxation per acre of farmland. Column (3) uses prefecture-level per capita taxation based on the 1776 population. Because historical administrative boundaries and population data are unavailable at the county level, the tax rate and per capita taxation measures are constructed at the prefecture level. Finally, column (4) replaces the continuous tax rate with an indicator for above-median tax burden, providing a specification that is less sensitive to measurement error and easier to interpret. Across all specifications, the triple interaction term is positive and statistically significant, indicating that—conditional on trade costs to Canton—regions with heavier tax burdens experienced larger increases in conflict when silver prices rose.

These effects are economically meaningful. A one-standard-deviation increase in silver price

Table 5: Heterogeneous Effects by Tax Burden

	$Conflicts_{it}$			
	Tax Rate	Tax Per Farmland	Tax Per Capita	1(Tax Rate > Median)
	(1)	(2)	(3)	(4)
$TradeCanton_i \times \Delta Silver_t \times Tax_i$	0.2126*	0.2258**	0.3144**	0.6361**
	(0.1107)	(0.0894)	(0.1488)	(0.3183)
$TradeCanton_i \times \Delta Silver_t$	12.5979***	11.8978***	9.2929***	11.4636***
	(3.8910)	(3.7526)	(3.5506)	(3.6041)
Baseline Controls	Yes	Yes	Yes	Yes
$Distance_i \times \Delta Silver_t$	Yes	Yes	Yes	Yes
County FE, Year FE	Yes	Yes	Yes	Yes
Observations	35496	32040	35208	36180
Pseudo R-squared	0.365	0.315	0.352	0.362

Notes: This table reports results using alternative measures of tax burden: prefecture-level tax rate (total taxes divided by historical agricultural potential), county-level taxation per acre of farmland, prefecture-level per capita taxation (based on the 1776 population), and an indicator for above-median prefecture-level tax burden. Because historical administrative boundaries and population data are unavailable at the county level, the tax rate and per capita taxation measures are constructed at the prefecture level. Controls follow those in Table 2, column (3). All tax measures except the indicator specification in column (4) are log-transformed. Standard errors clustered at the prefecture level are reported in parentheses. *** $p < 0.01$, ** $p < 0.05$, * $p < 0.1$.

growth (0.03) implies that, at median trade costs to Canton (8.17), a county at the 75th percentile of tax burden experiences approximately 8.5–11.2% more conflicts than a county at the 25th percentile, depending on the measure used: 11.2% under the tax rate specification (column 1), 8.5% under taxation per farmland (column 2), and 9.7% under per capita taxation (column 3). Under the binary specification in column (4), a one-standard-deviation increase in silver price growth implies approximately 16.9% more conflicts in counties with above-median tax burdens relative to counties below the median, evaluated at median trade costs to Canton.

3.4 Governmental Response to the Silver Shortage

Before turning to the theory section, we ask one further question: did the Qing state recognize the silver crisis, and how did it respond? Table 6 provides suggestive evidence.

Column (1) replicates the baseline specification using an indicator for receiving central government disaster relief or a tax exemption as the dependent variable. The positive and significant coefficient on $TradeCanton_i \times \Delta Silver_t$ suggests that counties more exposed to the silver shortage were indeed more likely to receive targeted relief when silver prices rose. Qing officials therefore appear to have recognized the regional incidence of the crisis and attempted to direct assistance

Table 6: Governmental Response to the Silver Shortage

	$I(\text{Exemption}_{it} + \text{Relief}_{it})$	log(Gov. Income$_t$)	log(Gov. Expenditure$_t$)	log(Exemp.$_t$ + Relief$_t$)
	(1)	(2)	(3)	(4)
$TradeCanton_i \times \Delta\text{Silver}_t$	1.2597***			
	(0.2651)			
ΔSilver_t		-0.3884***	-0.2420***	-2.8765***
		(0.1066)	(0.0787)	(0.3383)
Baseline controls	Yes	No	No	No
$\text{Distance}_i \times \Delta\text{Silver}_t$	Yes	No	No	No
County FE, Year FE	Yes	No	No	No
Observations	54540	79	79	178
R^2	0.247	0.116	0.059	0.329

Notes: Column (1) replicates Table 2, column (3), but uses an indicator for receiving relief from the central government or being granted a tax exemption as the dependent variable. Columns (2)–(4) use a time-series dataset to examine the relationship between the silver price and the Qing government's logged income and expenditures, as well as the logged annual frequency of relief and tax exemptions. Coefficients are estimated using an OLS model; standard errors, clustered at the prefecture level, are reported in parentheses. Significance levels: *** $p < 0.01$, ** $p < 0.05$, * $p < 0.1$.

toward the hardest-hit areas.

At the aggregate level, however, the government's response moved in the opposite direction. Column (4) shows that the total frequency of relief grants and tax exemptions actually declined when silver prices rose, precisely when demand for assistance was increasing. Columns (2) and (3) help explain why: rising silver prices coincided with sharp contractions in both government revenue and expenditure. As discussed in Section 2.2, silver-denominated taxes became increasingly difficult to collect as silver prices rose, while rigid fiscal institutions forced expenditures to adjust to declining revenues. Under the state's expenditure hierarchy—where military payrolls and official salaries took priority—relief transfers to the population were likely the primary margin of adjustment.

The Qing state was thus trapped by its own institutions. Rising silver prices simultaneously increased the real tax burden on ordinary households and weakened the state's fiscal capacity to respond. Rather than cushioning the external monetary shock, the silver-based fiscal system amplified economic hardship and left the dynasty poorly equipped for the deeper crises that followed.

Taken together, our empirical results yield three main findings. First, contractions in global silver supply led to rising silver prices within China, with larger increases in regions facing higher

trade costs to Canton. Second, these price changes had real consequences: counties with higher trade costs to Canton experienced significantly higher incidences of social unrest following increases in silver prices. Third, fiscal institutions amplified these effects: conditional on trade costs to Canton, regions facing heavier nominal tax burdens were more vulnerable to the silver shortage and exhibited larger increases in conflict. We also find suggestive evidence that the Qing state's rigid fiscal structure limited its ability to respond to the crisis, potentially further amplifying the social costs of the silver shock. In the next section, we develop a quantitative spatial model with silver trade and taxation to rationalize the main findings and conduct counterfactual analyses.

4 Theory

We now introduce a quantitative model that connects trade, silver circulation, and taxation. The framework rationalizes our empirical findings by showing how disruptions to foreign silver inflows generated uneven regional silver scarcities, amplified local fiscal pressure, and ultimately heightened the risk of unrest. It also provides the basis for the quantitative exercises that follow.

4.1 Model

Production and Trade. There are N Chinese regions, indexed by $i, n = 1, ..., N$, each endowed with L_i identical and immobile labor. Each region i produces a single tradable variety and is its sole source. The rest of the world (RoW), indexed by $i = 0$, has silver mines that exogenously produce silver for trade with China each period.

Consumers have CES utility over varieties produced in China, with an elasticity of substitution σ. Each region has a single merchant that delivers the local variety to buyers in each region, incurring iceberg trade costs τ_{in}. Merchants must pay a fixed cost in terms of silver, $M(f) = \frac{1-(1-f)^{1-1/\lambda}}{1-1/\lambda}$, à la Arkolakis (2010) to reach a fraction f of buyers in a location, where the parameter $\lambda > 0$ captures the rising cost of reaching more buyers. Given this setup, the price of variety i in market n is $p_{in} = \frac{\sigma}{\sigma-1}\tau_{in}w_i/A_i$, where w_i and A_i denote the wage and productivity

of local labor, respectively. The optimal buyer to reach is

$$f_{in} = \max\left\{1 - \left[\frac{X_n}{\sigma}\left(\frac{p_{in}}{P_n}\right)^{(1-\sigma)}\right]^{-\lambda}, 0\right\}, \tag{1}$$

where X_n is the aggregate expenditure on varieties. Assuming f_{in} is always positive, the equilibrium bilateral trade flow is given by:

$$X_{in} = f_{in}\left(\frac{p_{in}}{P_n}\right)^{(1-\sigma)} X_n = \left(1 - \left[\frac{X_n}{\sigma}\left(\frac{p_{in}}{P_n}\right)^{(1-\sigma)}\right]^{-\lambda}\right)\left(\frac{p_{in}}{P_n}\right)^{(1-\sigma)} X_n, \tag{2}$$

where the price index is given by $P_n = \left(\sum_{i=1}^{N} f_{in} p_{in}^{(1-\sigma)}\right)^{\frac{1}{1-\sigma}}$.

Merchants are assumed to hoard their profits in silver rather than consume locally. This assumption is motivated by two considerations. First, merchants constituted a small share of the population, and the assumption is consistent with historical evidence of widespread silver hoarding during the Qing period. Second, the taxes considered in our empirical and quantitative analysis were primarily levied on farmers and workers rather than merchants. Consequently, the effects of monetary conditions on real activity operate primarily through the income and expenditures of labor. Under this assumption, the silver inflow to region i, Δm_i, equals foreign imports plus trade surplus from other Chinese regions:

$$\Delta m_i = \frac{\sigma - 1}{\sigma}\left(X_{i0} + \sum_{n=1}^{N} X_{in}\right) - \sum_{n=1}^{N} X_{ni}, \tag{3}$$

where X_{in} are given by equation (2). We let $X_0 \equiv S_0$ denote the exogenous silver inflow from RoW to Canton.

Money in Utility. We now introduce time and the value of money. The representative agent in region i is endowed with the L_i units of labor and, in each period t, has preferences given by:

$$\sum_{t=0}^{\infty} \beta^t \left[\ln c_{it} + \gamma \ln \frac{m_{it+1}}{P_{it}}\right], \tag{4}$$

where $\frac{m_{it+1}}{P_{it}}$ is the demand for real silver balances at time t, and P_{it} is the price of local consumption goods in terms of silver.

At time $t = 0$, the region is endowed with $m_{i0} > 0$ units of silver. At the beginning of each subsequent period $t > 0$, a fixed fraction δ of the existing silver stock depreciates and ceases to circulate due to loss, wear, or other factors. The region also receives a fixed inflow M_{it} from local silver mines and an additional inflow Δm_{it} from trade. It then pays a silver-denominated tax T_{it}, which we model as a claim on local goods by the imperial court.[16] The evolution of the money supply is thus given by: $m_{it+1} = (1-\delta)m_{it} + \Delta m_{it} + M_{it}$. In this context, the trade-based inflow Δm_{it} reflects silver acquired by exchanging current-period consumption opportunities with other regions and the rest of the world.

Inter-temporal allocations. Now we characterize allocations and prices in such an economy. The time t budget constraint of the representative agent is

$$c_{it} + \frac{m_{it+1}}{P_{it}} \leq \frac{(1-\delta)m_{it}}{P_{it}} + \frac{w_{it}L_{it}}{P_{it}} + \frac{M_{it}}{P_{it}} - \frac{T_{it}}{P_{it}}, \quad \forall\, t, \tag{5}$$

given $m_{i0} > 0$. Optimizing over $\{c_{it}, m_{it+1}\}$ to maximize inter-temporal utility subject to (5) yields the Euler equation:

$$\frac{1}{P_{it}\, c_{it}} = \frac{\gamma}{m_{it+1}} + \frac{(1-\delta)\beta}{P_{it+1}\, c_{it+1}}, \tag{6}$$

which equates the marginal cost of holding an additional unit of silver today with the marginal benefit of holding it into the next period, which consists of the liquidity value γ / m_{it+1} and the future consumption value net of depreciation.

Steady State Equilibrium. We focus on the steady-state equilibrium of the model. In steady state, all real variables—output, consumption, and real money balances—are constant over time. Since taxes are fixed in silver terms, for the silver stock to remain stationary under sustained inflows, depreciation must exactly offset new silver acquisition, pinning down the steady-state

[16] Conceptually, the government uses local tax revenues to purchase local consumption goods. Hence, T_{it}/P_{it} enters the budget constraint as a reduction in available consumption, while taxation does not directly affect the law of motion for regional silver balances. We consider the alternative assumptions as sensitivity checks in the quantitative section.

money stock:

$$m_i = (1-\delta)m_i + \Delta m_i + M_i \quad \Rightarrow \quad m_i = \frac{\Delta m_i + M_i}{\delta}. \tag{7}$$

Combining the steady-state money stock with the Euler equation and the household budget constraint yields two key equilibrium relationships. First, the silver-denominated wage satisfies:

$$w_i = \frac{\Delta m_i \left[\frac{1-(1-\delta)\beta}{\delta\gamma} + 1\right] + M_i \left[\frac{1-(1-\delta)\beta}{\delta\gamma}\right] + T_i}{L_i}, \tag{8}$$

which links wages to silver inflows, local mining, and fiscal obligations. Second, equilibrium real consumption is proportional to total silver acquisition:

$$X_i = P_i c_i = \frac{1-(1-\delta)\beta}{\delta\gamma}(\Delta m_i + M_i). \tag{9}$$

Equilibrium System. Now we characterize the general equilibrium of the economy. For all $i, n \in N$, equilibrium is defined by the following system of equations, which jointly determine optimal household behavior and goods market clearing across regions:

$$w_i = \frac{\Delta m_i[\frac{1-(1-\delta)\beta}{\delta\gamma} + 1] + M_i[\frac{1-(1-\delta)\beta}{\delta\gamma}] + T_i}{L_i}, \tag{10}$$

$$X_i = P_i c_i = \frac{1-(1-\delta)\beta}{\delta\gamma}(\Delta m_i + M_i), \tag{11}$$

$$\Delta m_i = \frac{\sigma-1}{\sigma}\left(X_{i0} + \sum_{n=1}^{N} X_{in}\right) - \sum_{n=1}^{N} X_{ni}, \tag{12}$$

$$X_{i0} = \left(1 - \left[\frac{S_0}{\sigma}\left(\frac{\frac{\sigma}{\sigma-1}\frac{\tau_{i0}w_i}{A_i}}{P_0}\right)^{(1-\sigma)}\right]^{-\lambda}\right)\left(\frac{\frac{\sigma}{\sigma-1}\frac{\tau_{i0}w_i}{A_i}}{P_0}\right)^{(1-\sigma)} S_0, \tag{13}$$

$$X_{in} = \left(1 - \left[\frac{X_n}{\sigma}\left(\frac{\frac{\sigma}{\sigma-1}\frac{\tau_{in}w_i}{A_i}}{P_n}\right)^{(1-\sigma)}\right]^{-\lambda}\right)\left(\frac{\frac{\sigma}{\sigma-1}\frac{\tau_{in}w_i}{A_i}}{P_n}\right)^{(1-\sigma)} X_n \quad for \quad n = 1, ..., N. \tag{14}$$

where $P_n = \left(\sum_{i=1}^{N} f_{in}(\frac{\sigma}{\sigma-1}\frac{\tau_{in}w_i}{A_i})^{(1-\sigma)}\right)^{\frac{1}{1-\sigma}}$ with $f_{in} = \left(1 - \left[\frac{X_n}{\sigma}\left(\frac{\frac{\sigma}{\sigma-1}\frac{\tau_{in}w_i}{A_i}}{P_n}\right)^{(1-\sigma)}\right]^{-\lambda}\right)$, and S_0 is the exogenous aggregate foreign silver supply. Given equations (13), (14), equations (10)–(14)

comprise $3 \times N$ equations in $3 \times N$ unknowns $\{w_i, \Delta m_i, X_i\}_{i \in N}$.

Definition 1 (Equilibrium). *Given parameters $(\delta, \beta, \gamma, \sigma, \lambda)$, RoW silver supply S_0, and regional characteristics $\{L_i, A_i, T_i, \tau_{i0}, \tau_{in}, M_i\}_{i,n \in N}$, the equilibrium of the economy consists of $\{w_i, \Delta m_i, X_i\}_{i \in N}$ such that: (i) wages $\{w_i\}$ satisfy (10); (ii) silver inflows $\{\Delta m_i\}$ satisfy (12), with bilateral trade flows determined by (13)–(14); and (iii) aggregate expenditures $\{X_i\}$ satisfy (11).*

4.2 The Aftermath of Silver Disruption

In this subsection, we use the model to analyze how a collapse in foreign silver supply generates heterogeneous regional changes in silver price and real consumption, and how these responses interact with local tax burdens to produce welfare losses. Throughout, we map conflict incidence to worker welfare, allowing for a negative but flexible relationship between the two. While the model does not explicitly endogenize conflict, this link is well suited to the localized and subsistence-driven nature of the unrest episodes in our data.[17]

For analytical clarity, we consider a simplified version of the model that abstracts from silver minting and interregional trade. These assumptions are broadly consistent with the limited role of domestic minting and the largely local consumption structure of Qing China. Under these conditions, equilibrium regional silver inflows are given by:

$$\Delta m_i = \frac{\sigma - 1}{\sigma} \left(1 - \left[\frac{S_0}{\sigma} \left(\frac{\frac{\sigma}{\sigma-1} \frac{\tau_{i0} w_i}{A_i}}{P_0} \right)^{(1-\sigma)} \right]^{-\lambda} \right) \left(\frac{\frac{\sigma}{\sigma-1} \frac{\tau_{i0} w_i}{A_i}}{P_0} \right)^{(1-\sigma)} S_0, \tag{15}$$

where S_0, as before, denotes the exogenous silver supply to China from the rest of the world. Equation (15) implies that reductions in foreign silver supply lower regional silver inflows. Moreover, these effects are amplified by trade costs τ_{i0}, so that remote regions experience disproportionately larger declines. We summarize these results in the following proposition:

[17] Couttenier et al. (2024) develop a quantitative spatial framework that jointly models trade and conflict, where conflict is shaped by bilateral frictions and the value of local resources. Their framework is particularly well suited to settings in which armed actors are mobile and fight over extractable surplus. By contrast, the unrest in our setting are highly localized, with participants typically remaining within their home counties (Section 2). These conflicts were less about capturing resources elsewhere than about resistance emerging when fiscal and rental pressures pushed households below subsistence levels (Bernhardt, 1992). Given the localized and subsistence-driven nature of these conflicts, welfare changes provide a natural reduced-form mapping to conflict incidence, which we use to study the impact of counterfactual policy changes in Section 5.

Proposition 1. *The partial elasticity of silver inflow with respect to foreign supply is positive and increases with trade costs τ, that is, $\frac{\partial^2 \ln \Delta m_i}{\partial \ln S_0 \partial \ln \tau_{i0}} > 0$.*

How do heterogeneous regional silver inflows translate into local silver-price fluctuations? In the absence of interregional trade, local consumption prices move proportionally with silver-denominated wages. Equation (8) therefore implies that regions experiencing larger declines in silver inflows also experience larger declines in local consumption prices relative to silver—that is, a greater appreciation of silver relative to local consumption bundles. This corresponds to our first empirical finding and is summarized in Proposition 2:

Proposition 2. *When aggregate foreign silver supply declines, regions with higher trade costs to Canton experience greater appreciation of silver relative to local consumption bundles.*

How do these regional silver-price fluctuations translate into welfare changes? Equations (10) and (11) imply that the representative agent's welfare can be written as:

$$\ln \omega_i = (1+\gamma) \ln \frac{\sigma - 1}{\sigma} A_i L_i + \ln(k-1) - \gamma \ln \delta + (1+\gamma) \ln \frac{\Delta m_i}{k \Delta m_i + T_i}, \tag{16}$$

where $k \equiv \frac{1-(1-\delta)\beta}{\delta\gamma} + 1 > 1$. Its partial elasticity with respect to $\ln \Delta m_i$ is given by:

$$\frac{\partial \ln \omega_i}{\partial \ln \Delta m_i} = (1+\gamma) \left(1 - \frac{k \Delta m_i}{k \Delta m_i + T_i} \right). \tag{17}$$

The elasticity is positive and increasing in T_i, implying that regions with higher fiscal burdens experience larger welfare losses following declines in silver inflows.[18] Considering that conflict incidence is negatively correlated with welfare changes of workers, this finding matches our empirical findings 2 and 3, which we summarize in the following proposition:

Proposition 3. *When aggregate foreign silver supply declines, regions with higher trade costs to Canton experience greater welfare declines and, consequently, higher conflict incidence. The effect is more pronounced when the local tax burden is high.*

To better understand how trade geography and taxation jointly deliver these results, we highlight two points. First, the spatial heterogeneity in trade costs is crucial for generating differenti-

[18] In Appendix C, we provide comparative statics analyses accounting for general equilibrium effects and demonstrate that the results remain valid under mild regularity conditions.

ated regional responses. Canton's unique position as China's sole authorized treaty port—located at the southernmost periphery—created particularly acute silver scarcities in interior provinces. Had international trade been more dispersed across multiple ports, the welfare costs of silver supply disruptions would have been distributed more evenly, potentially attenuating conflict incidence. In the limiting case where all regions face identical trade costs, Proposition 2 implies uniform price changes that leave no scope for the spatial variation we document empirically.

Second, trade disruptions alone do not generate welfare losses in the absence of fiscal obligations. As shown in equation (16), welfare is independent of silver inflows when silver-denominated taxes are zero ($T_i = 0$). Once general-equilibrium effects are taken into account, a decline in foreign silver supply would in fact increase welfare, as more consumption varieties remain in the domestic market (Appendix C). Silver-denominated fiscal obligations are therefore the key mechanism through which silver scarcity translates into local economic distress.

This interaction between monetary and fiscal channels also explains why relatively modest trade disruptions generated disproportionately large social consequences. In standard trade models, welfare losses arise through reduced consumption possibilities or diminished export demand (Arkolakis et al., 2012, 2019). Yet international commerce accounted for only a small share of China's GDP in the early nineteenth century, implying limited direct exposure to foreign trade shocks. Nor can money-demand considerations alone explain the magnitude of the effects, since rural households transacted primarily in copper cash rather than silver, and wages and goods prices denominated in copper did not experience comparably large fluctuations over the period. The fiscal channel was therefore central: increases in silver's purchasing power translated directly into higher real tax burdens. In a predominantly agrarian economy where households earned income largely in kind and held little savings, even moderate increases in real fiscal pressure could push vulnerable households below subsistence thresholds and trigger unrest.

5 A Thirst for Silver: Quantification

Building on the equilibrium system developed in Section 4.1, we calibrate and estimate the key parameters using historical data from the period preceding the Spanish American wars of independence. We calibrate the model to 249 Qing prefectures, taking 1810 as the baseline year. We

use the calibrated framework to quantify the welfare consequences of the observed silver supply disruption. We then evaluate the relative importance of different transmission channels and assess whether alternative trade or tax policies could have mitigated the adverse effects of the silver shock.

5.1 Taking the Model to Data

Calibrated parameters. We calibrate the structural parameters as follows. We set the trade elasticity to $\sigma - 1 = 4$, following Simonovska and Waugh (2014). The annual silver depreciation rate is set to $\delta = 1.7\%$, capturing physical wear and loss as in Boehm and Chaney (2024). We set the discount factor to $\beta = 0.96$, following Kydland and Prescott (1982). The trade cost parameter λ, which captures frictions in accessing buyers, is typically calibrated between 0.915 (Arkolakis, 2010) and 1.1 (Eaton et al., 2011); for computational simplicity, we set $\lambda = 1$. We discipline the money-demand parameter γ using historical estimates of silver stocks and living costs. Around 1800, China's population was approximately 330 million, while annual living costs averaged about 4–5 taels of silver per person. Lee (2010) estimate that silver in circulation at the beginning of the nineteenth century totaled roughly 338 million taels. These values imply:

$$\gamma = (1 - (1 - \delta)\beta)\,\frac{m}{PC} = (1 - (1 - 0.017) \cdot 0.96) \cdot \frac{3.38}{3.30 \cdot 4.5} \approx 0.01. \tag{18}$$

Population, taxation, and silver stocks. Regional population data ($\{L_i\}$) are drawn from Cao (2001), and tax data ($\{T_i\}$, land and head taxes) come from Guo (2022), both for 1820, the closest year available to 1810. We compute the 1810 silver stock using data from Lee (2010), who report stocks for 1776 and 1820 together with annual inflows and domestic production. We recover the implied 1810 stock by interpolating between the reported benchmark years using observed inflows, domestic production, and an assumed constant depreciation rate.

Parameterization of trade costs. We model bilateral trade costs $\{\tau_{in}\}$ as a function of the bilateral travel cost calculated from the geo-spatial model described in Section 2:

$$\ln(\tau_{in}) = \kappa_1^{F,H} + \kappa_2^{F,H} \ln(\text{TravelCost}_{in}) + \epsilon_{in}. \tag{19}$$

Following Eaton et al. (2011), we normalize $\tau_{nn} = 1$ for all n. Since the allocation of foreign silver inflows depends only on relative international trade costs across regions, κ_1^F is not separately identified and is therefore normalized to 1.

Parameterization of productivity. Regional productivity $\{A_i\}$ is parameterized as:

$$\ln(A_i) = \kappa_3 \ln(L_i) + \kappa_4 \ln(LandEndow_i) + \mathbf{D}_{\text{silk, tea, ceramic}} + \epsilon_i, \tag{20}$$

where L_i denotes population, $LandEndow_i$ captures a region's effective land endowment—defined as land productivity scaled by usable land area, and $\mathbf{D}_{\text{silk, tea, ceramic}}$ are indicator variables for regions producing tea, silk, and ceramics, the major export goods of the period.[19] Population data are taken from Cao (2001), effective land endowment is proxied using prefecture-level caloric output from Galor and Özak (2016), and the indicator variables are constructed from information in county gazetteers.

Domestic silver minting. To calibrate domestic silver production $\{M_{it}\}$, we use aggregate production data from Lin (2020) together with mine location information from Wei (1983). Lin reports national silver output in multi-year aggregates; we convert these totals into annual production by assuming constant output within each reporting interval and taking period averages. Wei (1983) documents the locations of silver mines. In the absence of more detailed production records, we allocate annual national output evenly across all prefectures documented as having mining sites. Silver output between 1800 and 1840 was minimal, averaging less than 0.05% of the total stock in circulation. Accordingly, our estimates are unlikely to be sensitive to alternative allocation assumptions.

Targeted regional price variation. Direct measures of regional GDP or wages are unavailable for this period, but the Qing administration systematically collected monthly grain prices in silver terms across prefectures and grain types. To our knowledge, these data provide the broadest geographic coverage of prices available for early nineteenth-century China. We therefore estimate the remaining structural parameters by targeting cross-regional variation in a grain-based

[19] The model only identifies productivity up to a common multiplicative constant. Uniform proportional changes in productivity affect prices and real consumption but leave nominal equilibrium allocations unchanged.

Table 7: Determinants of Trade Costs and Technology

	ln Trade Cost		ln Technology		Model Fit	
	International	Domestic				
ln Travel Cost	0.23	0.11	ln Population	−0.92	ln P_i^{model}	1.07**
Constant		0.16	ln Agri. Yield	0.01		(0.51)
			Production: Tea	0.02		
			Production: Silk	0.09	R-squared	0.83
			Production: Ceramic	0.04	Observations	247

Notes: Parameters are estimated by minimizing the within-province sum of squared deviations between ln P_i^{grain} and ln $P_i^{model}(\kappa)$, controlling for province fixed effects. The Model Fit column reports the coefficient from regressing ln P_i^{grain} on ln P_i^{model} with province fixed effects. Standard errors in parentheses. ** $p < 0.05$.

consumption price index, P_i^{grain}. Specifically, we use data from 1800–1810 and estimate:

$$\ln(P_{igt}) = D_i + D_g + D_t + \epsilon_{igt}, \tag{21}$$

where P_{igt} is the reported price of grain g in prefecture i at month t, and D_i, D_g, and D_t denote prefecture, grain-type, and month fixed effects, respectively. The estimated prefecture fixed effects, $\exp(\hat{D}_i)$, serve as our measure of the grain-based consumption price index across regions. After removing variation due to grain type and temporal fluctuations, the remaining prefecture-specific component captures regional differences in food prices. Since food accounted for the bulk of household consumption during this period, the resulting index provides a natural proxy for regional variation in consumption costs.

5.2 Estimates and Model Validation

We estimate the parameters governing trade costs and productivity by minimizing the within-province sum of squared deviations between ln P_i^{grain} and the model-implied price index, ln P_i^{model}. Province fixed effects absorb broad regional differences in price levels unrelated to the model, such as persistent differences in food preferences or agricultural specialization.

Table 7 reports the coefficients. For international trade, the elasticity of trade costs with respect to travel costs is 0.23, which corresponds to a trade elasticity of 0.92. This value is very close to modern estimates, such as the mean distance elasticity of 0.93 reported in the meta-analysis by Head and Mayer (2014). For domestic trade, we find a smaller elasticity, indicating that bilat-

Table 8: Regional Variation in Silver Prices

	Untargeted Margins				Replicate Fact 1	
	Data		Model		Model (1800, 1810, 1840)	
	(1)	(2)	(3)	(4)	(5)	(7)
	$\ln Silver_{1810}$	$d \ln Silver_{1810-1840}$	$\ln Silver_{1810}$	$d \ln Silver_{1810-1840}$	$\Delta Silver_{it}$	$\Delta Silver_{it}$
$TradeCanton_p$	0.06**	0.03	0.06***	0.0004***	0.0104***	0.0341***
	(0.03)	(0.02)	(0.00)	(0.0001)	(0.0022)	(0.0029)
$TradeCanton_p \times MexicoSilver_t$					-0.0006***	-0.0020***
					(0.0001)	(0.0002)
$MexicoSilver_t$					-0.5853***	-0.5897***
					(0.0011)	(0.0011)
Baseline Controls					No	Yes
Observations	17	14	249	249	498	498
R-squared	0.27	0.18	0.84	0.04	1.00	1.00

Notes: This table presents regression results examining the relationship between trade with Canton and silver prices across different specifications. Columns (1)-(2) show results using raw data, columns (3)-(4) present model-based estimates, and columns (5) and (7) replicate the empirical findings for the period 1800-1840. Column (7) includes baseline controls. Standard errors are reported in parentheses. Significance levels: *** $p < 0.01$, ** $p < 0.05$, * $p < 0.1$.

eral trade decays less rapidly within countries than across international borders. This pattern is broadly consistent with empirical evidence that distance matters more for trade across nations (e.g., Anderson and Van Wincoop (2003)).

Turning to technology, the estimated elasticity of productivity with respect to population is -0.92, implying that population growth reduces output per worker and yields only marginal gains in total output.[20] This result accords with Lewis's classic insight that traditional agricultural sectors are characterized by surplus labor and low marginal productivity (Lewis, 1954). Meanwhile, caloric potential and endowments in tea, silk, and ceramics are positively associated with labor productivity, highlighting the importance of favorable land characteristics and specialized cash crops for regional productivity advantages.

We evaluate the model's external validity by comparing model-implied silver prices—both in levels and changes—to the data. Since neither silver price levels nor their changes were used in the calibration, this exercise serves as an external validity check. Table 8 reports the results. The model predicts that regions farther from Canton exhibit higher silver price levels in 1810 (column 3), consistent with the data (column 1). Extending the calibration to 1840, the model also reproduces the positive correlation between silver price increases and travel cost to Canton (column 4 vs. column 2).[21] In columns 5–6, we solve for equilibrium silver prices relative to

[20]The estimate implies that a 1% increase in population raises total output $A \times L$ by only $1 - 0.92 = 0.08\%$.

[21]Specifically, from the 1810 equilibrium, we impose the observed aggregate silver inflow decline between 1810

local consumption for 1800, 1810, and 1840, which allows us to replicate the Fact 1 regression with and without baseline controls. The model performs well qualitatively: regions more distant from Canton experience larger *increases* in silver price growth when Mexican silver production *declines*. Although the model is not intended to capture all sources of variation in silver prices, it successfully reproduces the central empirical patterns.

5.3 Welfare Effects and Policy Counterfactuals

We now quantify the general equilibrium effects of the global silver disruption and assess the extent to which domestic policy reforms could have mitigated its adverse impacts. Our analysis proceeds in three steps. First, we simulate the historical silver supply shock by imposing a 16.4% decline in equilibrium silver stocks, corresponding to historical estimates that China lost about 16.4% of its silver stock between 1808 and 1856 (Lin, 2020). Second, we decompose the resulting welfare changes to identify the quantitative contributions of three transmission channels. Third, we evaluate three counterfactual policy reforms— two trade liberalizations and tax redistribution—and examine how each would have shaped the economy's adjustment to the global silver shock.

Real effects of world silver disruption. Table 9 reports the baseline counterfactual results. The top panel summarizes percentage changes in key aggregate outcomes following the historical silver shock. The population-weighted average welfare loss is 1.16%, but the effects are highly uneven across space, with losses ranging from negligible in some regions to as large as 4.11% in the most adversely affected inland prefectures. This pronounced spatial heterogeneity reflects differences in exposure to international trade and, more importantly, in the burden of silver-denominated tax obligations across regions.

The silver price (relative to local consumption bundles) increases by roughly 41% on average, reflecting the sharp contraction in the money supply. These price movements generate substantial real consumption losses, particularly in regions where tax liabilities account for a large share of income. After-tax real wages fall by about 1.15% on average. As shown in the middle panel of Table 9, the silver shock raises the effective tax burden—defined as tax payments relative to

and 1840 as an exogenous shock, then solve for the resulting equilibrium prices for 1840.

Table 9: Welfare, Prices, and Tax Burden

	Pop.wt. Mean	SD	Max	Min
Panel A: Percentage Changes in Aggregate Outcomes				
Welfare	−1.158	0.817	−0.001	−4.114
Silver Price	41.154	0.140	41.355	40.645
After-Tax Real Wage	−1.147	0.809	−0.001	−4.074
Panel B: Tax Burden Before and After Silver Shock				
Before	0.022	0.015	0.074	0.000
After	0.033	0.023	0.111	0.000

Panel C: Welfare Decomposition (Population-Weighted)

	Total	Money Holding	Consumption	Taxation
Welfare Change (%)	−1.158	−0.011	0.003	−1.150
Share of Total (%)	100.00	0.99	−0.28	99.29

Notes: This table presents the welfare effects of a 16.4% decline in silver stocks. Panel A reports population-weighted mean percentage changes together with dispersion statistics across 249 prefectures. Panel B compares tax burden levels (measured as tax payments relative to income) before and after the silver shock. Panel C decomposes the population-weighted average welfare change into three components: real money balance effects, direct consumption effects, and taxation effects. The share row reports each component's contribution to the total welfare change. Values reported as 0.000 reflect magnitudes below the rounding threshold and are not exact zeros.

income—from 2% to 3% on a population-weighted basis. In the most heavily taxed prefectures, the burden rises from 8% to 11%—a more than three-percentage-point increase, which in levels exceeds the economy-wide average pre-shock tax burden. This amplification occurs because taxes are fixed in nominal silver terms, while incomes decline in silver terms as the price of silver rises.

Decomposing welfare effects across channels. To identify the mechanisms driving aggregate welfare losses, we use the household utility function to decompose log welfare into three components: utility from real money balances (money holding), consumption absent tax liabilities, and the welfare cost of taxation. Formally:

$$\ln \text{Welfare}_i = \underbrace{\gamma \ln\left(\frac{m_i}{P_i}\right)}_{\text{Money Holding}} + \underbrace{\ln\left(\frac{w_i L_i - \delta m_i}{P_i}\right)}_{\text{Consumption}} + \underbrace{\left[\ln\left(\frac{w_i L_i - \delta m_i - T_i}{P_i}\right) - \ln\left(\frac{w_i L_i - \delta m_i}{P_i}\right)\right]}_{\text{Taxation}}. \tag{22}$$

The decomposition isolates (i) the welfare change arising from shifts in real money balances, (ii) the change in real consumption in the absence of taxation, and (iii) the residual effect attributable to taxation.

The bottom panel of Table 9 reports the decomposition. Strikingly, the taxation channel ac-

counts for 99.29% of the total welfare loss. The real money balance effect is negative (-0.01), indicating that silver holdings declined more sharply than local prices, but its quantitative contribution is small, representing only 0.99% of the total loss. The direct consumption effect is slightly positive, as reduced foreign silver inflows leave more output available for domestic consumption, but its contribution is negligible (-0.28%), consistent with China's low degree of trade openness in this period.

The overwhelming dominance of the taxation channel underscores the central role of fiscal rigidity in transmitting the global silver shock to the Chinese economy. Because tax obligations were fixed in nominal silver terms and could not be readily adjusted, the sharp rise in silver prices mechanically increased the real tax burden on households. In regions where initial tax rates were already high, this fiscal tightening imposed large welfare costs by compressing consumption, which in turn contributed to rising local unrest. This mechanism also helps explain why the silver shock generated large and spatially uneven impacts despite China's limited integration into world markets. While trade exposure shaped the geographic distribution of the shock, fiscal rigidity determined its quantitative severity: the interaction of an external monetary contraction with silver-denominated tax obligations amplified welfare losses, particularly in remote or fiscally vulnerable regions.

Alternative policy scenarios. Were the consequences of the silver shock inevitable, or could any policy reform have prevented it from becoming the cause of state fragility? This question directly speaks to long-standing debates in Chinese economic history over whether the crises of the nineteenth century reflected the costs of restrictive trade institutions, the rigidity of fiscal institutions, or deeper constraints beyond the reach of feasible policy reform.

Historians have long debated the role of the Canton system in China's nineteenth-century decline. Some scholars view the system as a closed-door policy that limited beneficial global integration, while revisionists argue that it was economically efficient and that China's difficulties reflected other institutional rigidities (Pomeranz, 2000). Fiscal institutions have been similarly debated. One influential view downplays taxation as a source of distress because Qing tax rates were remarkably low by international standards—around 2–3% of output, or 5–10% when all forms of collections are included, compared with 15–20% in contemporary European states (Wang, 1973;

Table 10: Policy Counterfactuals: Trade and Tax Reforms

	Direct Effect				Post-Reform Silver Shock			
	Mean	SD	Max	Min	*Mean*	SD	Max	Min
	(1)	(2)	(3)	(4)	(5)	(6)	(7)	(8)
Panel A: Trade Reform (Four-Port System)								
Welfare Change (%)	0.052	0.130	1.050	−0.139	−1.130	0.792	−0.001	−4.155
Panel B: Trade Reform (Treaty Port System)								
Welfare Change (%)	0.045	0.106	0.746	−0.255	−1.134	0.799	−0.001	−4.179
Panel C: Tax Reform (Equal Per Capita Tax)								
Welfare Change (%)	0.708	1.551	6.208	−1.505	−0.781	0.002	−0.778	−0.788

Notes: This table presents welfare effects from three counterfactual policy reforms. Panel A reports results for a trade liberalization that reopens four major ports (Ningbo, Zhangzhou, Songjiang, and Canton) for international trade, compared to the baseline Canton-only system. Panel B reports results for a trade liberalization that opens the 14 treaty ports established after the First and Second Opium Wars (excluding the Taiwan ports of Tainan and Danshui). For both trade reforms, international trade costs are set to the minimum cost of reaching any of the open ports. Panel C presents a fiscal reform that equalizes per capita tax payments across all prefectures while holding aggregate tax revenue constant. For each reform, columns (1)–(4) report the direct effect of implementing the reform from the 1810 baseline, and columns (5)–(8) show the welfare effect of the 16.4% silver stock shock after the reform is in place. Statistics reported are population-weighted means together with dispersion measures across the 249 prefectures.

Wong, 1997). Our model nevertheless highlights two features that this comparison misses: the spatial inequality of tax burdens and the rigidity of silver-denominated obligations.

Motivated by these debates, we evaluate three counterfactual reforms: (i) a return to the pre-Canton four-port system; (ii) a treaty-port system resembling the trade regime China was forced to adopt after the Opium Wars;[22] and (iii) a fiscal reform that equalizes per capita tax payments across regions. We focus on these reforms because they were institutionally conceivable within the Qing administrative framework, though actual implementation would have involved practical constraints. While our analysis does not settle these broader historical controversies, it provides quantitative evidence on which margins of policy adjustment would have most effectively reduced the welfare costs of an external monetary shock. Table 10 presents the results.

Panel A of Table 10 reports the first counterfactual, a return to the pre-Canton era when international trade was permitted through four major ports: Ningbo, Zhangzhou, Songjiang, and Canton. We implement this reform by lowering each region's international trade cost to the min-

[22]The treaty-port system refers to the ports opened to foreign trade under the treaties following the First Opium War (Treaty of Nanjing, 1842) and the Second Opium War (Treaties of Tianjin, 1858, and Convention of Beijing, 1860). It comprised sixteen ports: Canton, Zhangzhou, Fuzhou, Ningbo, Songjiang, Niuzhuang, Dengzhou, Tainan, Danshui, Chaozhou (Shantou), Qiongzhou, and the riverine ports of Wuchang, Jiujiang, Jiangning, Zhenjiang, and Tianjin. We exclude Tainan and Danshui because both lie on Taiwan.

imum cost of reaching any of the four ports. Column 1 shows that the reform itself generates a modest direct welfare gain of 0.05%, with heterogeneous effects across prefectures. When the silver shock subsequently hits, the population-weighted welfare loss is −1.13% (column 5), slightly *smaller* than under the baseline Canton system (−1.16%), and the cross-regional dispersion of losses also narrows (the standard deviation falls from 0.82 to 0.79). The intuition is that opening additional ports gives foreign silver more points of entry into the economy, so the global contraction is transmitted more evenly across space rather than concentrated in regions distant from Canton, easing the spatial variation in silver scarcity. The mitigating effect is nonetheless small: the reform does nothing to offset the aggregate decline in silver inflows and only reshapes their spatial allocation.

Panel B considers a more far-reaching liberalization: opening the fourteen treaty ports that China was compelled to open after the Opium Wars. Qualitatively, the results resemble those of the four-port reform. The direct welfare gain is again modest (column 1), and the subsequent silver shock produces a loss of −1.13% (column 5). Notably, opening fourteen ports does *not* outperform opening four: the direct gain is slightly smaller (0.045% versus 0.052%), and the post-shock loss is marginally larger (−1.134% versus −1.130%). This pattern illustrates a general second-best principle (Lipsey and Lancaster, 1956; Bhagwati and Ramaswami, 1963; Bai et al., 2024): in an economy with multiple coexisting distortions, relaxing one friction more aggressively need not raise welfare. Extending trade access well beyond the four historical ports further redistributes silver inflows toward the coast, leaving some interior prefectures more—not less—exposed when the global contraction arrives, which partly offsets the direct gains from reduced trade costs.

Panel C turns to the fiscal reform, which equalizes per capita tax payments across all prefectures while holding aggregate tax revenue constant. The direct welfare effect is substantial: a population-weighted gain of 0.71% (column 1). This reflects both the efficiency gains from reducing spatial distortions and the progressive incidence of the reform, which benefits populous regions that initially bore high tax burdens. Crucially, when the silver shock occurs after the reform (column 5), the welfare loss is only −0.78%—about a third smaller than the baseline (−1.16%). Moreover, the cross-regional dispersion of losses nearly vanishes (the standard deviation falls to essentially zero), indicating that all regions experience similar proportional declines. This is exactly what the welfare decomposition predicts: because the tax channel dominates wel-

Table 11: From Welfare to Conflict: Predicted Conflict Incidence under Counterfactual Scenarios

	No Disaster Controls				With Disaster Controls			
	1801-1810	1831-1840	$\Delta Conflicts$	% of obs. rise	1801-1810	1831-1840	$\Delta Conflicts$	% of obs. rise
	(1)	(2)	(3)	(4)	(5)	(6)	(7)	(8)
Observed (data)	134.1	237.9	+103.8	—	134.1	237.9	+103.8	—
Baseline shock	143.5	228.5	+85.0	81.9%	145.4	236.9	+91.5	88.2%
Four ports	143.5	222.7	+79.2	76.3%	145.4	230.6	+85.2	82.1%
Treaty ports	143.5	223.5	+80.0	77.0%	145.4	231.5	+86.1	82.9%
Tax equalization	143.5	148.8	+5.3	5.1%	145.4	151.1	+5.7	5.5%

Notes: This table maps the structural welfare changes into changes in conflict incidence in the data. Columns (1)–(3) and (5)–(7) report predicted average annual conflict events across the 249 prefectures: the predicted 1810 level, the predicted post-shock (or post-reform-plus-shock) level, and their difference. Columns (4) and (8) express the predicted change as a share of the observed rise in average annual conflict between 1801–1810 and 1831–1840 (+103.8 events), measuring the portion attributable to the silver shock through welfare rather than overall model fit; the remainder reflects climatic, demographic, and other factors. Columns (1)–(4) use the no-control specification ($\hat{\beta} = -0.197$, s.e. 0.108); columns (5)–(8) additionally control for local disasters (drought, flood, hail, frost, snow), held at pre-shock values in prediction ($\hat{\beta} = -0.213$, s.e. 0.138). The mapping is a back-of-the-envelope exercise rather than a causal estimate.

fare changes, heterogeneous tax burdens are the primary source of spatial heterogeneity in the adjustment to the silver shock. If unrest incidence rises as welfare declines, such compression in the distribution of losses could translate into a substantial reduction in overall unrest.

From welfare to conflict incidence. The welfare results above speak directly to one of the central questions motivating this paper: how much of the rise in local unrest during this period can be attributed to the global silver disruption interacting with institutional rigidity? In the final part of this section, we provide a simple back-of-the-envelope mapping. Specifically, we regress changes in prefecture-level per capita conflict frequency on model-implied changes in log welfare between 1810 and 1840. To mitigate concerns that the benchmark years may reflect idiosyncratic shocks, we use ten-year averages ending in each benchmark year. The estimated elasticity is -0.197 (s.e. 0.108), confirms a negative relationship between welfare changes and unrest, which we then apply to each counterfactual welfare path to obtain predicted conflict counts.

Table 11 reports the results. Columns (1) to (4) report the baseline specification, while Columns (5) to (8) additionally control for natural disasters when estimating the welfare–conflict relationship. In the data, annual conflict incidence rose sharply between the first and third decades of the nineteenth century, from 134 to 238 events. The estimated relationship implies a fitted conflict level of 143 events in the first decade, close to the observed 134. Following the observed silver shock, predicted annual conflict incidence rises to 229 events, an increase of 85 events that

accounts for roughly 82% of the observed rise in unrest. Controlling for local natural disasters leaves the estimated contribution of the silver shock, if anything, slightly larger at 88%, suggesting that the results are not driven by climatic shocks coinciding with the silver contraction.

Turning to counterfactual policy changes, the two trade liberalizations leave the predicted increase in conflict largely intact, still explaining 76–77% of the observed rise. By contrast, equalizing per capita tax payments compresses the predicted increase dramatically: the silver-attributable rise in conflict falls from 85 to just 5 events per year, reducing the explained share from 82% to roughly 5%. This suggests that, had the Qing government implemented fiscal reform in response to the external silver shock, the resulting rise in conflict would have been negligible.

6 Conclusion

This paper provides the first systematic empirical evidence that rigid trade and taxation systems, combined with a global decline in silver production triggered by the Spanish American Wars of Independence, fueled social instability in early nineteenth-century Qing China. Drawing on newly assembled county-level panel data and a novel dataset on historical commercial routes, we show that regions farther from Canton—the empire's sole international port—faced sharper silver price increases and higher conflict incidence following the silver supply shock. Moreover, conditional on trade costs to Canton, heavier nominal tax burdens amplified this relationship. We develop a quantitative spatial model incorporating silver trade and taxation to rationalize these findings. Quantitative estimates indicate that the global silver shock lowered China's aggregate welfare by 1.16%, with the tax channel accounting for most of the loss. Contrary to the common narrative that greater trade openness would have benefited late imperial China, opening additional international ports would have had only a modest mitigating effect. By contrast, fiscal reform emerges as a far more effective policy lever.

Taken together, the findings of the paper make several contributions to the literature. First, to our knowledge, this is one of the first studies to provide systematic evidence on the mechanisms through which the nineteenth-century silver shortage translated into social conflict in Qing China, a connection long discussed by historians but never rigorously tested. Second, we integrate reduced-form empirical analysis with a quantitative spatial model, allowing us not only to

document causal relationships, but also to quantify welfare effects, decompose mechanisms, and evaluate counterfactual policies—a combination that, to our knowledge, has not been applied in either economic history or the broader trade and conflict literature. Finally, our findings speak to a question of first-order importance in today's world: under what conditions can global integration become a source of state fragility? Our results suggest that institutional rigidity can be a critical choke point. Even in a relatively closed economy, an external shock can generate large welfare losses and political instability when mediated by rigid domestic institutions, a finding that resonates with contemporary debates over trade decoupling, sanctions, and supply-chain fragility.

References

AHLFELDT, G. M., S. J. REDDING, D. M. STURM, AND N. WOLF (2015): "The Economics of Density: Evidence from the Berlin Wall," *Econometrica*, 83, 2127–2189.

ANDERSON, J. E. AND E. VAN WINCOOP (2003): "Gravity with Gravitas: A Solution to the Border Puzzle," *American Economic Review*, 93, 170–192.

ARKOLAKIS, C. (2010): "Market Penetration Costs and the New Consumers Margin in International Trade," *Journal of Political Economy*, 118, 1151–1199.

ARKOLAKIS, C., A. COSTINOT, D. DONALDSON, AND A. RODRÍGUEZ-CLARE (2019): "The Elusive Pro-Competitive Effects of Trade," *The Review of Economic Studies*, 86, 46–80.

ARKOLAKIS, C., A. COSTINOT, AND A. RODRÍGUEZ-CLARE (2012): "New Trade Models, Same Old Gains?" *American Economic Review*, 102, 94–130.

BAI, Y., X. BIAN, AND R. JIA (2025): "Endogenous Canal: How Did National Capital Relocation Reshape Economic Geography in Historical China?" Unpublished manuscript.

BAI, Y., K. JIN, AND D. LU (2024): "Misallocation under Trade Liberalization," *American Economic Review*, 114, 1949–1985.

BAI, Y. AND J. K.-S. KUNG (2018): "A Reversal of Trade Fortune: Opium, Silver, and the Decline of Late Imperial China, 1789–1910," Working Paper.

BERMAN, N., M. COUTTENIER, D. ROHNER, AND M. THOENIG (2017): "This Mine Is Mine! How Minerals Fuel Conflicts in Africa," *American Economic Review*, 107, 1564–1610.

BERNHARDT, K. (1992): *Rents, Taxes, and Peasant Resistance: The Lower Yangzi Region, 1840–1950*, Stanford, California: Stanford University Press.

BHAGWATI, J. AND V. K. RAMASWAMI (1963): "Domestic Distortions, Tariffs and the Theory of Optimum Subsidy," *Journal of Political Economy*, 71, 44–50.

BOEHM, J. AND T. CHANEY (2024): "Trade and the End of Antiquity," CEPR Discussion Paper 19459, CEPR Press, Paris & London.

BORAH, W. W. (1949): "The Mining Guild of New Spain and Its Tribunal General 1770-1821," .

BRZEZINSKI, A., Y. CHEN, N. PALMA, AND F. WARD (2024a): "The Vagaries of the Sea: Evidence on the Real Effects of Money from Maritime Disasters in the Spanish Empire," *The Review of Economics and Statistics*, 106, 1220–1235.

BRZEZINSKI, A., N. PALMA, AND F. R. VELDE (2024b): "Understanding Money Using Historical Evidence," *Annual Review of Economics*, 16, 571–595.

CAO, S. (2001): *Zhongguo renkoushi (Qing shiqi) (The Population History of China (Qing Dynasty))*, Shanghai: Fudan University Press, (in Chinese).

CAO, S., Y. LI, AND B. YANG (2012): "Mt. Tambora, Climatic Changes, and China's Decline in the Nineteenth Century," *Journal of World History*, 587–607.

CAO, Y. AND S. CHEN (2022): "Rebel on the Canal: Disrupted Trade Access and Social Conflict in China, 1650–1911," *American Economic Review*, 112, 1555–1590.

COUTTENIER, M., J. MARCOUX, T. MAYER, AND M. THOENIG (2024): "The Gravity of Violence," CEPR Discussion Paper 19527, CEPR Press, Paris & London.

DAI, Y. (2019): *The White Lotus War: Rebellion and Suppression in Late Imperial China*, University of Washington Press.

DELL, M., B. FEIGENBERG, AND K. TESHIMA (2019): "The Violent Consequences of Trade-Induced Worker Displacement in Mexico," *American Economic Review: Insights*, 1, 43–58.

DONALDSON, D. (2018): "Railroads of the Raj: Estimating the Impact of Transportation Infrastructure," *American Economic Review*, 108, 899–934.

DONALDSON, D. AND R. HORNBECK (2016): "Railroads and American Economic Growth: A "Market Access" Approach," *Quarterly Journal of Economics*, 131, 799–858.

DU, S., S. HE, AND G. HUANG (2024): "Jinrong fazhan cujin le shichang yitihua ma: laizi qingdai piaohao sheli yu liangshi shichang de zhengju (Financial Development Promotes Market Integration: Evidence from Piaohao Establishment and Grain Market in the Qing Dynasty)," *China Economic Quarterly*, 24, 1085–1102, (in Chinese).

EATON, J., S. KORTUM, AND F. KRAMARZ (2011): "An Anatomy of International Trade: Evidence from French Firms," *Econometrica*, 79, 1453–1498.

FANG, Z., Z. JIANG, ET AL. (1996–2014): *Guangdong tongshi (General History of Guangdong (Six Volumes))*, Guangzhou: Guangdong Higher Education Press, 1st ed., (in Chinese).

FEARON, J. D. AND D. D. LAITIN (2003): "Ethnicity, Insurgency, and Civil War," *American Political Science Review*, 97, 75–90.

FEUERWERKER, A. (1980): "Economic Trends in the Late Ch'ing Empire, 1870–1911," in *The Cambridge History of China, Volume 11: Late Ch'ing, 1800–1911, Part 2*, ed. by J. K. Fairbank and K.-c. Liu, Cambridge University Press, 1–69.

FISHER, I. (1933): "The Debt-Deflation Theory of Great Depressions," *Econometrica*, 1, 337–357.

FOGEL, R. W. (1964): *Railroads and American Economic Growth: Essays in Econometric History*, Baltimore: Johns Hopkins Press.

GALOR, O. AND Ö. ÖZAK (2016): "The Agricultural Origins of Time Preference," *American Economic Review*, 106, 3064–3103.

GUO, Y. (2022): *Land and Labor Tax in Imperial Qing China (1644-1912)*, vol. 18, Brill.

HE, P. (2008): *Qingdai fuishui zhengce yanjiu (Studies on Qing Dynasty Taxation Policy)*, Beijing: China Social Sciences Press, (in Chinese).

HEAD, K. AND T. MAYER (2014): "Gravity Equations: Workhorse, Toolkit, and Cookbook," in *Handbook of International Economics*, Elsevier, vol. 4, 131–195.

HO, P.-T. (1959): *Studies on the Population of China, 1368–1953*, Cambridge, MA: Harvard University Press.

HORNBECK, R. AND M. ROTEMBERG (2024): "Growth Off the Rails: Aggregate Productivity Growth in Distorted Economies," *Journal of Political Economy*, 132, 3547–3602.

HU, Y. (2021): "Qingdai yinqian bijia bodong yanjiu (1644–1911) (Research on the Exchange Rate Fluctuation between Silver and Copper Coin in the Qing Dynasty (1644–1911))," Ph.D. thesis, East China Normal University, Shanghai, (in Chinese).

HUANG, P. C. (1990): *The Peasant Family and Rural Development in the Yangzi Delta, 1350-1988*, Stanford, California: Stanford University Press.

JONES, S. M. AND P. A. KUHN (1978): "Dynastic Decline and the Roots of Rebellion," in *The Cambridge History of China, Volume 10: Late Ch'ing, 1800–1911, Part 1*, ed. by J. K. Fairbank, Cambridge University Press, 107–162.

JUHÁSZ, R. (2018): "Temporary Protection and Technology Adoption: Evidence from the Napoleonic Blockade," *American Economic Review*, 108, 3339–3376.

KING, F. H. (1965): *Money and Monetary Policy in China, 1845–1895*, Harvard University Press.

KUHN, P. A. (1990): *Soulstealers: The Chinese Sorcery Scare of 1768*, Cambridge, MA: Harvard University Press.

KUNG, J. K.-S. AND C. MA (2014): "Can Cultural Norms Reduce Conflicts? Confucianism and Peasant Rebellions in Qing China," *Journal of Development Economics*, 111, 132–149.

KYDLAND, F. E. AND E. C. PRESCOTT (1982): "Time to Build and Aggregate Fluctuations," *Econometrica: Journal of the Econometric Society*, 1345–1370.

LEE, L. (2009): "Estimating the Yearly Amount of Silver Inflow during the Ching Dynasty in China (1645-1911)," *Journal of Humanities and Social Sciences*, 5, 31–58.

——— (2010): *Qingdai de guoji maoyi: Baiyin liuru, huobi weiji he wanqing gongyehua (International Trade in the Qing Dynasty: Silver Inflows, Currency Crises, and Late Qing Industrialization)*, Taipei: Showwe Publishing, (in Chinese).

LEWIS, W. A. (1954): "Economic Development with Unlimited Supplies of Labour," *The Manchester School*, 22, 139–191.

LI, B. (2015): "The "Daoguang Depression" and the "Guiwei Great Flood": Economic Decline and Climatic Cataclysm in Early Nineteenth-Century Songjiang in a New Perspective," *Études chinoises*, 34, 89–119.

——— (2020): *An Early Modern Economy in China: The GDP of the Huating-Lou Area, 1820s*, Cambridge: Cambridge University Press.

LIN, M.-H. (2020): "China Upside Down: Currency, Society, and Ideologies, 1808–1856," in *China Upside Down*, Harvard University Asia Center.

LIPSEY, R. G. AND K. LANCASTER (1956): "The General Theory of Second Best," *The Review of Economic Studies*, 24, 11–32.

LIU, C.-Y. (1993): ""Chong, Fan, Pi, Nan": Qingdai Dao, Fu, Ting, Zhou, Xian dengji chutan ("Cong, Fan, Pi, Nan": A Preliminary Study of the Hierarchy of Circuits, Prefectures, Departments, Subprefectures, and Counties in the Qing Dynasty)," *Bulletin of the Institute of History and Philology, Academia Sinica*, 64, 175–204, (in Chinese).

MA, D. (2012): "Money and Monetary System in China in the 19th-20th Century: An Overview," Economic History Working Paper 159/12, London School of Economics and Political Science, Department of Economic History.

MARTIN, P., T. MAYER, AND M. THOENIG (2008): "Make Trade Not War?" *The Review of Economic Studies*, 75, 865–900.

MERRILL, C. W. AND STAFF OF THE COMMON METALS DIVISION (1930): "Summarized Data of Silver Production," Economic Paper 8, U.S. Department of Commerce, Bureau of Mines, Washington, D.C.

MORSE, H. B. (2007): *The Chronicles of the East India Company Trading to China, 1635–1834*, Folkestone: Global Oriental, (Originally published 1926–1929).

MYERS, R. H. AND Y.-C. WANG (2002): "Economic Developments, 1644–1800," in *The Cambridge History of China, Volume 9, Part 1: The Ch'ing Empire to 1800*, ed. by W. J. Peterson, Cambridge University Press, 563–645.

NAGY, D. K. (2023): "Hinterlands, City Formation and Growth: Evidence from the U.S. Westward Expansion," *Review of Economic Studies*, 90, 3238–3281.

PALMA, N. (2022): "The Real Effects of Monetary Expansions: Evidence from a Large-Scale Historical Experiment," *The Review of Economic Studies*, 89, 1593–1627.

PASCALI, L. (2017): "The Wind of Change: Maritime Technology, Trade, and Economic Development," *American Economic Review*, 107, 2821–2854.

PENG, X. (2020): *Zhongguo huobi shi (A Monetary History of China)*, Shanghai: Shanghai People's Publishing House, 4th ed., (in Chinese, originally published in 1958).

POMERANZ, K. (2000): *The Great Divergence: China, Europe, and the Making of the Modern World Economy*, Princeton: Princeton University Press.

REDDING, S. J. AND D. M. STURM (2008): "The Costs of Remoteness: Evidence from German Division and Reunification," *American Economic Review*, 98, 1766–1797.

RICHARDS, J. F. (2002): "The Opium Industry in British India," *The Indian Economic & Social History Review*, 39, 149–180.

SIMONOVSKA, I. AND M. E. WAUGH (2014): "The Elasticity of Trade: Estimates and Evidence," *Journal of International Economics*, 92, 34–50.

VAN DYKE, P. A. (2005): *The Canton Trade: Life and Enterprise on the China Coast, 1700–1845*, Hong Kong: Hong Kong University Press.

VICARD, V. (2012): "Trade, Conflict, and Political Integration: Explaining the Heterogeneity of Regional Trade Agreements," *European Economic Review*, 56, 54–71.

VON GLAHN, R. (2007): "Foreign silver coins in the market culture of nineteenth century China," *International Journal of Asian Studies*, 4, 51–78.

VON GLAHN, R. (2018): "Economic Depression and the Silver Question in Nineteenth-Century China," in *Global History and New Polycentric Approaches*, ed. by M. Perez Garcia and L. de Sousa, Singapore: Palgrave Macmillan, 81–118.

——— (2023): *Fountain of Fortune: Money and Monetary Policy in China, 1000–1700*, Berkeley: University of California Press.

WAKEMAN, F. J. (1978): "The Canton Trade and the Opium War," in *The Cambridge History of China, Volume 10: Late Ch'ing, 1800–1911, Part 1*, ed. by J. K. Fairbank, Cambridge University Press, 163–212.

WANG, Y.-C. (1973): *Land Taxation in Imperial China, 1750–1911*, Cambridge, MA: Harvard University Press.

——— (1981): *Zhongguo jindai huobi yu yinhang de yanjin (1644–1937) (The Evolution of Currency and Banking System in Modern China: 1644–1937)*, Taipei: Institute of Economics, Academia Sinica, (in Chinese).

——— (1997): "Shijiu shiji qianqi wujia xialuo yu taipingtianguo geming (Deflation and the Mass Peasant Uprisings in Mid-19th Century China)," in *Qingdai jingjishi lunwenji (Collected Essays in the Economic History of Qing China)*, Taipei: Linking Publishing, vol. 3, 417–448, (in Chinese).

WEI, Q. (1983): *Qingdai de kuangye (Mining in the Qing Dynasty. Volume 2)*, Beijing: Zhonghua Book Company, (in Chinese).

WONG, R. B. (1997): *China Transformed: Historical Change and the Limits of European Experience*, Ithaca: Cornell University Press.

ZHANG, D. (2013): *Zhongguo sanqiannian qixiang jiluzongji (A Comprehensive Collection of Meteorological Records of China over the Past 3000 Years)*, Nanjing: Jiangsu Education Press, (in Chinese).

Online Appendix for: "A Thirst for Silver: Trade Shock, Taxation, and Local Unrest in Nineteenth-Century China"

A Data Appendix

A.1 Estimating Trade Costs

In this subsection, we describe how we estimate trade costs using GIS data, historical archival sources, and geospatial methods.

The historical GIS data used in this study are sourced from the Harvard China Historical GIS project, which provides comprehensive spatial and administrative datasets for historical China (CHGIS, 2016b). We specifically use the 1820 dataset, which includes georeferenced vector data on hydrographic features (such as rivers, canals, and waterways), polygon shapefiles delineating provincial and prefectural boundaries, and point data representing county-level administrative units (CHGIS, 2016a). These spatial layers form the foundation for constructing business road networks and modeling travel paths in late imperial China.

In addition to historical GIS data, we incorporate elevation data from the Copernicus Digital Elevation Model (DEM), available through the Copernicus Data Space Ecosystem (European Space Agency, 2022). We use the *COP-DEM_GLO-90-DGED* dataset, which provides global elevation data at a $90 \times 90m^2$ spatial resolution. Derived from multiple contributing satellite missions, this dataset offers consistent, high-quality elevation coverage that is well-suited for geographic modeling.

A.1.1 Construction of Business Routes

This section describes the construction of historical business routes based on the *Shanggu Bianlan*. As detailed in the previous subsection, this Qing-era commercial travel guide records rich information on waypoint sequences for trade routes (e.g., from A through C, D, and E, to B), which we digitized and geofenced when possible. While the guide provides detailed travel information, it does not specify the actual travel paths between these waypoints. To better approximate historical travel conditions, we model the likely paths connecting these points using information on terrain and river systems to account for China's complex geographical constraints.

Starting from these digitized waypoint connections (undirected graphs), we employed least-cost path analysis using ESRI ArcGIS software to determine the most probable routes actually

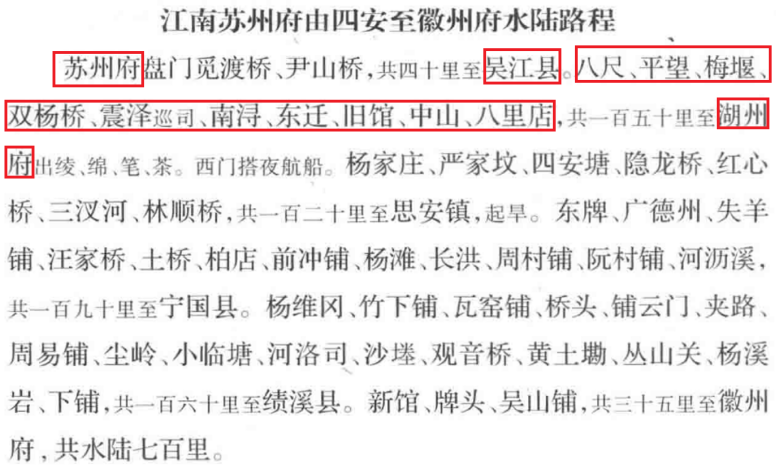
江南苏州府由四安至徽州府水陆路程

苏州府盘门觅渡桥、尹山桥，共四十里至吴江县。八尺、平望、梅堰、双杨桥、震泽巡司、南浔、东迁、旧馆、中山、八里店，共一百五十里至湖州府出绫、绵、笔、茶。西门搭夜航船。杨家庄、严家坟、四安塘、隐龙桥、红心桥、三汊河、林顺桥，共一百二十里至思安镇，起旱。东牌、广德州、失羊铺、汪家桥、土桥、柏店、前冲铺、杨滩、长洪、周村铺、阮村铺、河沥溪，共一百九十里至宁国县。杨维冈、竹下铺、瓦窑铺、桥头、铺云门、夹路、周易铺、尘岭、小临塘、河洛司、沙埭、观音桥、黄土墩、丛山关、杨溪岩、下铺，共一百六十里至绩溪县。新馆、牌头、吴山铺，共三十五里至徽州府，共水陆七百里。

Notes: This figure shows an example of a trade route documented in *Shangjubianlan* ("A Convenient Handbook for Merchants"). The illustrated route is from Suzhou to Huizhou via Si'an. Place names identified in the first sentence of the original text are highlighted in red boxes.S

Figure A1: Historical Trade Route Documentation from *Shangjubianlan*

traveled between each pair of consecutive waypoints. Our geospatial model adapts the calibration parameters from Scheidel and Meeks (2012) and Bai et al. (2025), adjusted specifically for early 19th-century Qing China transportation technology. This approach replaces the unknown—but often implicitly assumed straight-line connections—with more realistic travel routes based on time and cost minimization.

The cost structure reflects the technological and economic realities of pre-modern Chinese commerce, where waterborne transport enjoyed substantial advantages over overland alternatives. Natural waterways serve as the baseline $(1x)$, while the Grand Canal incurs a modest premium $(1.5x)$ due to traffic congestion, towing fees, and toll payments. For terrestrial routes, we adapted Tobler's hiking function to model the exponential increase in transport costs with terrain slope: road travel costs scale as $3 \times e^{3.5 \times |slope|} x$ for slopes $\leq$ 30%. This 30% slope threshold represents roughly the practical limit for mule-based cargo transport, the dominant overland freight method in early 19th-century China. Beyond this threshold, the cost function incorporates an additional penalty $(3 \times e^{3.5 \times 0.3 + 4 \times |excess\ slope|} x)$ to reflect the necessity of switching to human porters, which significantly increases both time and expense. This parameterization ensures that our model realistically captures the strong preference for waterway transport that characterized early 19th-century Chinese commercial networks, while accurately modeling the increasing difficulty and cost of traversing China's mountainous interior regions.

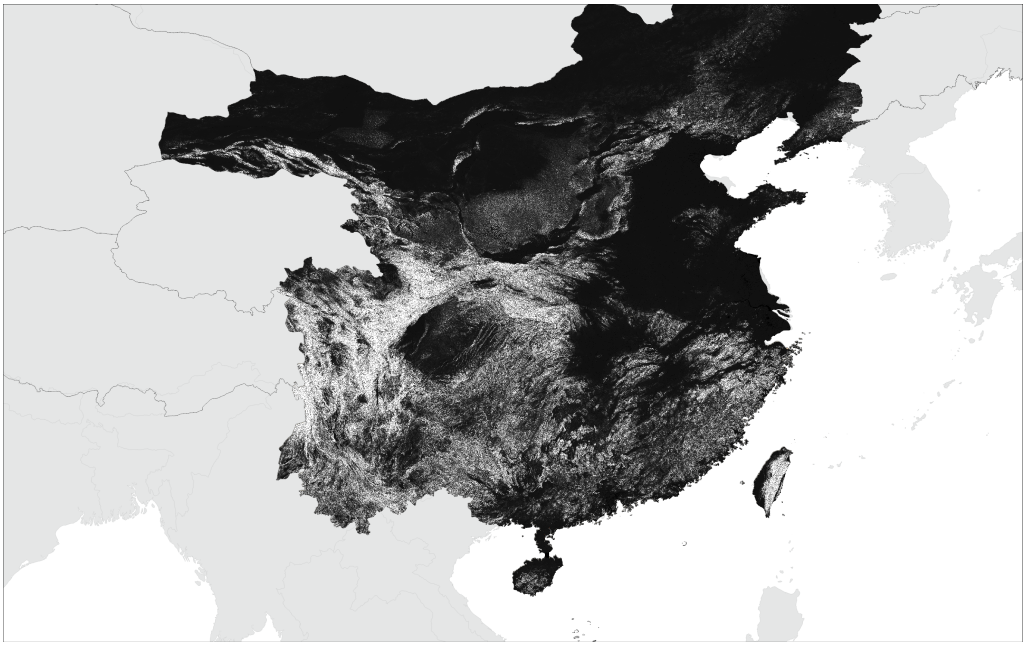

Notes: This figure shows the construction cost raster used as input for the least-cost path algorithm. The color scale ranges from white (indicating very high travel cost) to black (indicating very low travel cost). Cost values are determined based on land gradient (slope) and land cover (rivers, canals, and waterways) as described in more detail in the main text.

Figure A2: Construction Cost Raster

Adopting this geospatial model, we use remote sensing data on land cover and elevation, along with historical GIS data on hydrography described in the previous section, to construct a continuous cost surface across China Proper (the 18 Han Chinese regions). To ensure computational accuracy, we perform this analysis at the original resolution of the DEM data, using $90 \times 90m^2$ grid cells. This allows us to capture fine-grained topographical variations that can significantly influence historical transportation costs, particularly in China's mountainous regions where small changes in slope can dramatically affect travel feasibility and expense. Figure A2 provides a graphical illustration of the constructed cost surface, showing how transportation costs vary across the landscape according to our parameterized model.

We then proceed to construct the least cost paths between all 775 pairs of waypoints that we identified from Shanggu Bianlan. Using ArcGIS Spatial Analyst, we apply a raster-based Dijkstra's algorithm that first calculates cumulative cost distances from each origin point across the cost surface, then reconstructs optimal paths by tracing backward from destination points through the cost gradient. In the process, we also eliminate duplicate pair-wise connections that share identical start-end coordinates due to the use of county-level geographic references.[23] This

[23]When the original historical records specified locations such as village or port names, we geocoded these to

process ultimately enables us to construct 630 unique least-cost paths between the connected waypoint pairs identified from the Shanggu Bianlan, completing the construction of the historical business network.

A.1.2 Construction of the Least-Cost Path to Canton

The final step is to determine how counties are connected to Canton via the business network and to calculate the associated travel costs. While Canton is a node on the business network, 1,357 out of 1,561 counties are not directly connected to it, although most are located relatively close to the network. Given the difficulties of traveling along off-network trails in ancient China—such as poor road conditions, lack of service provisions, and security risks—we assume that merchants traveling from an off-network county to Canton would first connect to the nearest point on the established network whenever possible, and then follow the network routes to Canton via the least-cost path.

This approach breaks our computation into two parts. First, we identify the least-cost path from each off-network county to the business network using Dijkstra's algorithm, as applied in estimating the historical business routes. To ensure computational feasibility, we constrain the search area to a rotated rectangular extent extending approximately 55 km (0.5 degrees) in all directions from the straight-line path between each county and its nearest network point.[24] The second part involves calculating the least-cost path from the connection point to Canton along the established network, using the same cost-minimization principles.[25]

Following Bai et al. (2025), we assume that off-network trails incur a cost multiplier of 6 to

their corresponding county coordinates due to the difficulty of precisely locating the exact historical place. This county-level geocoding resulted in some route segments sharing identical start-end coordinates, creating apparent duplications that were consolidated during analysis.

[24]This buffer is economically justified by the spatial distribution of off-network counties: according to our calculations, approximately 1,200 out of 1,561 counties lie within 150 km of the network, so the 55 km extent provides a sufficient buffer (over 30%) to accommodate terrain-based detours. For the remaining counties located in remote mountainous areas, this search radius corresponds on average to roughly 15–20 days of travel, making it unlikely that any economically viable detour would extend beyond this boundary. We tested a subsample of data points using 1- and 2-degree extents and found no substantial change in results.

[25]Sea travel was very limited for internal commerce during our study period due to China's extensive inland river networks providing more reliable and cost-effective transportation than coastal routes. Our spatial model allows for coastal travel and sea crossings, assuming costs equivalent to natural waterway travel. To avoid multiple equilibria, for 15 counties located in Taiwan and Hainan, where maritime connections were essential for mainland access, we assume they are connected to the network using the shortest straight lines.

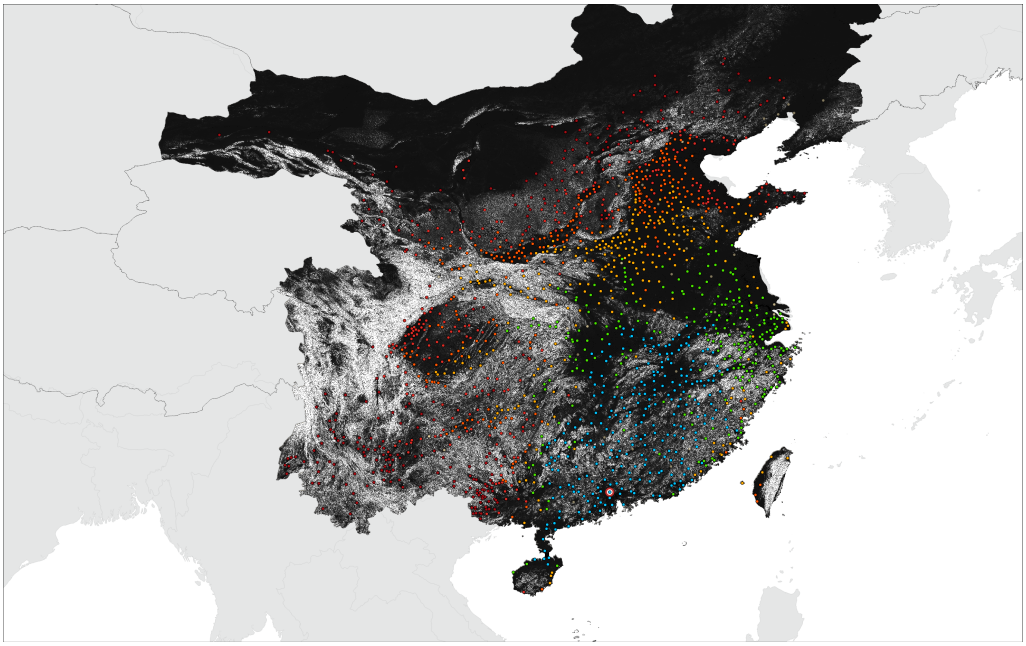

Notes: This figure overlays county locations onto the cost raster shown in Figure A2. Each county point is colored according to its calculated trade cost to Canton ($TradeCanton_i$): green/blue points indicate lower costs, while orange/red points indicate higher costs.

Figure A3: County Trade Costs to Canton

reflect poor road conditions and security risks.[26] Accordingly, the total travel cost to Canton for county i is computed as:

$$TradeCanton_i = 6 \times Cost_i^{OffNetwork} + Cost_i^{OnNetwork}$$

where $Cost_i^{OffNetwork}$ is the calculated off-network travel cost and $Cost_i^{OnNetwork}$ is the on-network cost from the connection point to Canton.

Figure A3 overlays county points onto the constructed cost raster, with point colors indicating our calculated travel costs to Canton (i.e., $TradeCanton_i$, using the same scale as Figure A2). The visualization illustrates a clear relationship between geography and trade costs. First, travel costs generally increase with distance from Canton. Second, counties located in mountainous regions or separated from Canton by difficult terrain—indicated by lighter shades on the raster—tend to have higher costs (red and orange points). In contrast, counties in flatter areas or without major geographic barriers show lower costs (green and blue points). Finally, counties located near or along established trade networks tend to have lower travel costs; this is perhaps best seen in the

[26] In robustness checks, we also consider alternative cost multipliers ranging from 1 to 10.

North China Plain, where counties exhibit travel costs to Canton comparable to those of some geographically closer counties in Guangxi with similar terrain conditions. This spatial pattern supports the validity of our cost calculation methodology.

A.1.3 Bilateral Trade Costs and Trade Costs to Silver Mines

Our analysis requires two additional sets of trade cost measures beyond the baseline trade costs to Canton. First, for the counterfactual exercises on trade reform (Section 5), we compute trade costs from each prefecture to four major ports: Canton, Ningbo, Zhangzhou, and Songjiang. For each destination, we apply the same methodology used for Canton, combining off-network and on-network components to identify the least-cost path. Because the quantification is conducted at the prefecture level, we aggregate county-level costs to the prefecture–port level using simple averages of constituent counties. Travel within the same prefecture is assumed of zero trade cost.

Second, for the empirical analysis, we also construct trade cost measures to the nearest silver mine in order to partition regions by their access to domestic silver production and coinage facilities. Unlike major ports, many mines lie in remote areas far from the established business network. In such cases, the baseline requirement that travelers first reach the network can generate implausible routes. For example, a county located close to a remote mine but far from the network may be assigned a highly indirect path running through the network rather than a realistic direct route.

To accommodate these cases, we allow fully off-network travel whenever it is cost-minimizing. Computing exact off-network least-cost paths for all county–mine pairs using the raster-based algorithm is computationally heavy; we therefore adopt an approximation strategy. For each county, we compute the ratio of its actual travel cost to the business network to its straight-line distance to the network, and use this terrain-adjusted multiplier to approximate the cost of a direct off-network path to each mine or mint. For each county–mine (or county–mint) pair, we then take the minimum of this approximated off-network cost and the through-network cost obtained from the baseline method. This procedure preserves computational feasibility while delivering more plausible cost estimates for destinations where off-network travel is likely optimal. Because these measures are used only to divide our data sample into two groups, any measurement error arising from this approximation is unlikely to materially affect our results.

A.2 Silver Prices

We use two sources of silver price data in our empirical analysis. For most specifications, we rely on the nationwide silver price series constructed by Lin (2020), which spans 1720–1911. Because the Qing state did not maintain official silver price records, the series is compiled from heterogeneous historical documents reporting local market prices. However, for our sample period (1801–1840), the underlying observations come from a single source: the ledger of a large chain store in Zhili province, where the capital Beijing was located. This consistency is advantageous for our empirical design. While regional silver prices may differ in levels or volatility, available evidence suggests that major market centers such as Beijing broadly shared the common temporal pattern of silver price movements across Qing China. Accordingly, regional differences in price changes are introduced by interacting this price change with each region's distance to Canton. Silver prices are quoted relative to copper, reflecting the Qing dynasty's bimetallic monetary system.[27]

To examine spatial heterogeneity in silver price responses to aggregate silver supply shocks, we also draw on the provincial silver price panel compiled by Hu (2021). This dataset, assembled from a broad range of archival sources, provides an unbalanced panel for 18 Han provinces from 1644 to 1911. For our study period, it contains 279 province-year observations. Because missing values are substantial—especially in the earlier decades—we rely primarily on the time-series from Lin (2020) in our main analysis, using the provincial panel only when cross-regional variation is required.

A.3 Silver Production and Foreign Silver Inflows

We use Mexico's annual silver coin production as an exogenous source of variation in China's silver supply. Production data are sourced from Borah (1949), who compiled comprehensive records from colonial Spanish and later Mexican mint archives. For years prior to 1821, Borah (1949) provides separate records for Mexico's annual production of silver and gold coins, distinguishing between the two metals. For the period after 1821—following Mexico's independence

[27] Silver prices are missing for 1815 and 1819, so these years are excluded from the analysis.

from Spain—only the combined total production of silver and gold coins is reported. To address this data limitation, we adjust the post-1821 series using the gold-silver production ratio observed during the pre-independence period (1801-1821). Mexico dominated global silver production during this period, accounting for approximately two-thirds of world output in the early nineteenth century, making its production shocks highly relevant for global silver markets and, consequently, for China's silver supply.

Data on China's silver inflows are obtained from Lee (2009), who estimates annual net silver flows by synthesizing customs records from European countries and their Asian colonies, supplemented with Chinese maritime trade documentation. During our sample period (1801–1840), Canton accounted for 93.2% of China's net silver inflow, underscoring the port's overwhelmingly dominant role in foreign silver trade and justifying our focus on trade costs to Canton as the key measure of exposure to international silver markets.

A.4 Conflict Data

Our measure of social *conflict* is the annual frequency of unrest reported in each county, sourced from the *Qingshilu* (Veritable Records of the Qing Dynasty). The *Qingshilu* constitutes the official chronicle of the Qing court, compiled from court diaries, memorials, and edicts, and provides systematic coverage of local disturbances reported to the central government (Kuhn, 1990). The dataset distinguishes three types of conflicts: banditry or other forms of resistance against legitimate authority (*fei ni*), tax resistance (*kang zu kang shui*), and riots during relief distribution (*qiang mi nao zhen*). Among these, banditry—typically involving disputes among commoners, theft, and various forms of localized violence—constitutes 93.6% of all recorded conflicts.

Several notes apply to interpreting these data. First, most recorded incidents represent small-scale, localized disturbances rather than large-scale rebellions. Unlike the major uprisings that dominate the conflict literature on modern civil wars (Fearon and Laitin, 2003), these events typically involved dozens or at most hundreds of participants and were contained within county boundaries. They are better characterized as routine social unrest or petty criminality than as organized political violence. Second, the *Qingshilu*'s categorization reflects official perspectives and political incentives rather than objective classification of events (Kuhn, 2002). Local officials faced strong incentives to downplay tax-related unrest. Admitting that peasants rebelled against

taxation could be interpreted as evidence of administrative failure or excessive extraction, potentially jeopardizing an official's career (Sng, 2014). In contrast, reporting incidents as "banditry" deflected blame onto lawless elements of society and justified requests for additional resources to maintain order (Ni and Van, 2006). Consequently, many incidents motivated by fiscal grievances were likely recorded as banditry, blurring the distinction between these categories. Given the reporting incentives and the conceptual overlap between categories, we do not distinguish among the three types in our empirical analysis. Instead, we interpret the aggregate conflict measure as capturing general social instability and local unrest.

A.5 Tax Data

We measure historical tax burdens using three alternatives that combine county-level aggregate tax obligations with different denominators. For the numerator, we use data from Guo (2022), who compiled comprehensive records of total land-and-poll taxes (*diding*) at the county level for various years throughout the Qing period. We select the 1760 tax data—the closest available year prior to our sample period—to minimize endogeneity concerns. These data represent official tax collections: fixed nominal obligations denominated in silver taels that remained largely unchanged over time. Importantly, they capture de jure tax burdens rather than de facto collections, which often included informal surcharges (Ni and Van, 2006). The relative stability of official collection over our sample period makes them arguably more exogenous than actual tax extractions, which could respond endogenously to local economic conditions.

To measure the tax burden imposed on local households, we consider three different denominators. First, we construct a measure of *tax rates* by dividing total tax obligations by potential agricultural income. To estimate agricultural income, we draw on agricultural suitability data from the Global Agro-Ecological Zones (GAEZ) project (Food and Agriculture Organization of the United Nations (FAO) and International Institute for Applied Systems Analysis (IIASA), 2021). For each CHGIS 1820 prefecture, we calculate the maximum potential value of agricultural output under pre-modern cultivation technology and use this as the denominator.[28] Second, we compute *tax per unit of farmland* by dividing total tax obligations by cultivated land area. Farm-

[28]CHGIS 1820 historical county-level shapefiles are not available, preventing us from spatially matching county-level GAEZ agricultural suitability data or performing more granular population estimates at the county level.

land data come from the 1933 agricultural census compiled by East Asia Research Institute (1943), which reports county-level cultivated acreage. Third, we calculate *tax per capita* using prefecture-level population in 1776—the closest year to the 1760 tax data—from Qing administrative records (Cao, 2001). Because agricultural income and population denominators exist only at the prefecture level, the associated tax measures are also calculated at that level.

A.6 Additional Data Sources

This subsection summarizes the additional data used in the analysis as empirical controls and in robustness exercises.

Political and Military Importance. During the Qing dynasty, counties were classified by the central government according to four criteria of administrative significance: *Chong* (transportation hub), *Fan* (administratively complex), *Pi* (fiscally distressed), and *Nan* (difficult to govern or insecure). These classifications were established in 1728, and we obtain the data from the *Qingshilu*.

Social Norms. We proxy the strength of local social norms using the number of genealogies dated to periods prior to 1750. Genealogy data come from the *Comprehensive Catalogue of Chinese Genealogies* (Wang, 2008) and are matched to counties using geographic coordinates.

Geographic Variables. Longitude and latitude of county administrative centers are drawn from the CHGIS 1820 dataset (CHGIS, 2016a). County-level average elevation is computed from the NOAA GLOBE (NOAA, 1999). Agricultural suitability, measured in caloric potential, is from Galor and Özak (2016). Because CHGIS 1820 provides point locations but no boundary shapefiles, we construct county polygons using Thiessen (Voronoi) methods to compute spatial averages.

Domestic Mines and Mints. Locations of silver mines are obtained from Wei (1983).

Other Controls. Annual county-level frequencies of *natural disasters*—droughts, floods, frosts, hail, and snow—are compiled from the *Comprehensive Gazetteer of Chinese Meteorological Disasters* (Zhang, 2013). Indicators for key export commodities (ceramics, silk, tea) are drawn from county gazetteers. *Opium trade* is measured using the annual series on India's opium exports to China reported in Richards (2002). An indicator for whether a prefecture lies along the Grand Canal

comes from Cao and Chen (2022), and an indicator for whether a province was affected by the White Lotus Rebellion (1796–1804) is obtained from Dai (2019).

A.7 Variable Definitions and Summary Statistics

Finally, Table A1 reports the definitions, data sources, and construction of all variables used in the empirical analysis. Unless otherwise noted, variables in the provincial-level regressions are computed as the arithmetic mean of their constituent counties or prefectures whenever such aggregation is feasible.

Table A1: Data Source and Variable Description

Variable Name	Data Description	Data Source	Observations	Mean	S.D.
Conflict					
$conflict_{it}$	Conflict frequency	Qing Shilu	54540	0.1153	0.8746
Silver Price					
$Silver_t$	Time series silver price (relative to copper)	Lin (2020)	38	1241.3947	203.3897
$\Delta Silver_t$	Time series log change rate of silver price (relative to copper)	Lin (2020)	36	0.0105	0.0305
$Silver_{pt}$	Panel series silver price (relative to copper)	Hu (2021)	280	1225.5464	197.4670
$\Delta Silver_{pt}$	Panel series log change rate of silver price (relative to copper)	Hu (2021)	190	0.0116	0.0525
Foreign Silver Supply					
$Inflow_t$	Annual silver inflow (Unit: ten million tales)		112	0.1155	0.2501
$MexicoSilver_t$	Log annual silver coin production of Mexico (Unit: number of coins)	Borah (1949), see A.3 for interpolation method	120	2.8526	0.0221
Trade Cost with Canton					
$TradeCanton_i$	Log travel cost to Canton (Unit: cost of traveling 1 km via natural waterways within the network)	See A.1	1515	8.0727	0.7029
$TradeCantonSL_i$	Log travel cost to Canton, assuming uniform travel costs (Unit: km)	See A.1	1515	7.3269	0.6239
Baseline Controls					

Continued on next page

Data Source and Variable Description

Variable Name	Data Description	Data Source	Observations	Mean	S.D.
$Distance_i$	Log distance to Canton (Unit: km)	Calculated by GIS	1515	6.8871	0.6205
$Drought_{it}$	Log annual frequency of drought	Zhang (2013)	54540	0.0259	0.1361
$Flood_{it}$	Log annual frequency of flood	Zhang (2013)	54540	0.0362	0.1655
$Hail_{it}$	Log annual frequency of hail	Zhang (2013)	54540	0.0026	0.0433
$Frost_{it}$	Log annual frequency of frost	Zhang (2013)	54540	0.0014	0.0317
$Snow_{it}$	Log annual frequency of snow	Zhang (2013)	54540	0.0019	0.0373
$Norm_i$	Log number of genealogies recorded no later than 1750	He (2008), matched according to geographical coordinates, county range interpolated by Tyson polygon	1515	1.3917	1.5006
$Chong_i$	Indicator of being *Chong*	Liu (1993)	1515	0.3558	0.4789
Fan_i	Indicator of being *Fan*	Liu (1993)	1515	0.4092	0.4919
Pi_i	Indicator of being *Pi*	Liu (1993)	1515	0.1888	0.3915
Nan_i	Indicator of being *Nan*	Liu (1993)	1515	0.4502	0.4977
$Altitude_i$	Log average altitude (Unit: m)	Calculated by GIS software, with data from NOAA (1999), county range interpolated by Tyson polygon	1515	5.5109	1.5636
$Longitude_i$	Log longitude	CHGIS (2016a)	1515	4.7279	0.0488
$Latitude_i$	Log latitude	CHGIS (2016a)	1515	3.4518	0.1681
$Suitability_i$	Log average agriculture suitability, measured in Caloric (Unit: hundred million caloric)	Calculated by GIS software, with data from Galor and Özak (2016), county range interpolated by Tyson polygon	1515	9.3277	0.7911
$Area_i$	Log area of administration zone (Unit: square kilometer)	Calculated by GIS software, county range interpolated by Tyson polygon	1515	21.3921	0.7957
Domestic Silver Access					

Continued on next page

Data Source and Variable Description

Variable Name	Data Description	Data Source	Observations	Mean	S.D.
$TradeSilverMine_i$	Log travel cost to cost minimizing silver mine	See Section A.1 for variable construction, and Wei (1983) for distribution of mines	1515	1663.2902	1209.6814
$DistanceSilverMine_i$	Log distance to the closet silver mine	Calculated by GIS, see Wei (1983) for distribution of mines	1515	485.4172	304.9866
Fiscal Capacity					
$I(relief_{it} + exemption_{it})$	Indicator of receiving relief or exemption	Qing Shilu	54540	0.1086	0.3112
$Gov.Income_t$	Log annual income of Qing government (Unit: tales)	Shi (2009)	79	16.3162	0.3287
$Gov.Expenditure_t$	Log annual income of Qing government (Unit: tales)	Shi (2009)	79	16.3499	0.2863
Trade Cost/Distance to Placebo Cities					
$TradePort_i$	Log average travel cost to Ningbo, Songjiang, Zhangzhou (Unit: cost of traveling 1 km via natural waterways within the network)	See A.1	1515	8.0235	0.6480
$TradeBeijing_i$	Log travel cost to Beijing (Unit: cost of traveling 1 km via natural waterways within the network)	See A.1 1515	8.0850	0.7484	
$TradeNanjing_i$	Log travel cost to Nanjing (Unit: cost of traveling 1 km via natural waterways within the network)	See A.1 1515	7.7819	0.8286	

Continued on next page

Data Source and Variable Description

Variable Name	Data Description	Data Source	Observations	Mean	S.D.
$DistancePort_i$	Log average distance to Ningbo, Songjiang, Zhangzhou (Unit: km)	Calculated by GIS	1515	6.8948	0.4757
$DistanceBeijing_i$	Log distance to Beijing (Unit: km)	Calculated by GIS	1515	6.8468	0.7713
$DistanceNanjing_i$	Log distance to Nanjing (Unit: km)	Calculated by GIS	1515	6.6358	0.6672
Additional Controls					
$GrandCanal_i$	Indicator of locating along the Grand Canal	Cao and Chen (2022)	1515	0.0865	0.2811
$Ceramic_i$	Indicator of producing ceramic	County Gazetteer	1515	0.1149	0.3189
$Silk_i$	Indicator of producing silk	County Gazetteer	1515	0.2211	0.4151
Tea_i	Indicator of producing tea	County Gazetteer	1515	0.3439	0.4752
$RouteIntensity_i$	Length of trade routes passing by divided by $Area_i$ (Unit: kilometer per square kilometer)	Calculated by GIS software, county range interpolated by Tyson polygon	1515	2.0818	3.0326
$Opium_t$	India's log opium export to China (Unit: boxes)	Richards (2002)	36	8.8875	0.7942
$WhiteLocus_i$	Indicator of being affected by the White Locus Rebellion	Dai (2019)	1515	0.2508	0.4336

B Empirical Appendix

Table B1: Relevance of Mexican Silver to Chinese Inflows and Silver Prices

	$\Delta Silver_t$ 1721-1911		$SilverInflow_t$ 1721-1840	
	(1)	(2)	(3)	(4)
$SilverInflow_t$	-0.0140**	-0.0141**		
	(0.0059)	(0.0058)		
$MexicoSilver_t$			0.1033***	0.1608***
			(0.0318)	(0.0502)
Year Linear Trend	No	Yes	No	Yes
Observations	180	180	120	120
R-squared	0.046	0.046	0.025	0.229

Notes: The variable $\Delta Silver_t$ represents the log change in silver prices relative to copper, calculated from Lin (2020); $SilverInflow_t$ is China's net silver inflow (in ten million taels) from Lee (2009); $MexicoSilver_t$ represents the log of Mexican silver production, based on Borah (1949). The data are time series and cover the period 1721 to 1911 for columns (1)–(2), and 1721 to 1840 for columns (3)–(4). Coefficients are estimated using OLS, with robust standard errors reported in parentheses: *** $p < 0.01$, ** $p < 0.05$, * $p < 0.1$.

Table B2: Robustness: Alternative Samples and Controls

	$Conflicts_{it}$						
	Full Sample					Excl. White Locus Rebellion Prov.	Excl. Guangdong Prov.
	(1)	(2)	(3)	(4)	(5)	(6)	(7)
$TradeCanton_i \times \Delta Silver_t$	10.2529***	8.9720**	10.1514***	9.9470**	11.2881***	9.4030**	10.0087***
	(3.6175)	(3.5464)	(3.8785)	(4.5005)	(3.5856)	(4.197)	(3.8370)
Baseline FEs and Controls	Yes	Yes	Yes	Yes	Yes	Yes	Yes
Grand Canal$_i \times I(t \geq 1826)$	Yes	No	No	No	No	No	No
Province-Year FE	No	Yes	No	No	No	No	No
$ExportGoods_i \times \Delta Silver_t$	No	No	Yes	No	No	No	No
$TradeRouteIntensity_i \times \Delta Silver_t$	No	No	No	Yes	No	No	No
$Opium_t \times TradeCanton_i$	No	No	No	No	Yes	No	No
Observations	36180	34282	36180	36180	36180	27612	33912
Pseudo R-squared	0.362	0.431	0.362	0.361	0.362	0.381	0.330

Notes: The dependent variable is the number of conflicts per county-year. This table replicates Table 2 regressions, adding controls or subsamples to test robustness. Column 1 adds an interaction between Grand Canal location and post-1826 years; column 2 includes province-year fixed effects; column 3 interacts export-good dummies (silk, tea, ceramics) with $\Delta Silver_t$; column 4 interacts trade route intensity with $\Delta Silver_t$; column 5 interacts log India opium exports to China with $TradeCost_i$; column 6 excludes provinces affected by the White Lotus Rebellion (Henan, Shaanxi, Sichuan, Hubei); column 7 excludes Guangdong province. See Data Appendix for variable construction details. Coefficients are from pseudo-Poisson models with prefecture-level clustered standard errors. Significance: * $p < 0.1$, ** $p < 0.05$, *** $p < 0.01$.

Table B3: Robustness: Alternative Measure of Travel Cost

	$Conflicts_{it}$		
	(1)	(2)	(3)
$TradeCanton_i \times \Delta Silver_t$	2.4040	5.4703**	8.9905***
	(2.1033)	(2.6162)	(3.4774)
Baseline Controls	No	No	Yes
$Distance_i \times \Delta Silver_t$	No	Yes	Yes
County FE, Year FE	Yes	Yes	Yes
Observations	36180	36180	36180
Pseudo R-squared	0.359	0.359	0.361

Notes: This table replicates the regressions reported in Table 2, but calculates travel costs to Canton without adapting to geospatial conditions—that is, using the shortest straight-line distances from counties to the road network and assuming straight-line links within the network. Coefficients are estimated using a pseudo-Poisson model, with standard errors clustered at the prefecture level shown in parentheses. Significance levels: *** $p < 0.01$, ** $p < 0.05$, * $p < 0.1$.

Table B4: Domestic Silver Supply Alleviates Social Unrest

	$Conflicts_{it}$			
	Travel Cost to Cost-minimizing Silver Mine		Straight Line Distance to nearest Silver Mine	
	Cost.≥medium	Cost.<medium	Dist.≥medium	Dist.<medium
	(1)	(2)	(3)	(4)
$TradeCanton_i \times \Delta Silver_t$	16.4754***	7.3352	15.0383***	5.3748
	(4.8362)	(4.4885)	(5.7250)	(4.7402)
Baseline Controls	Yes	Yes	Yes	Yes
$Distance_i \times \Delta Silver_t$	Yes	Yes	Yes	Yes
County FE, Year FE	Yes	Yes	Yes	Yes
Observations	17712	18468	18180	18000
Pseudo R-squared	0.314	0.408	0.322	0.414

Notes: The dependent variable is the number of conflicts for a given county and year. This table replicates the regressions reported in Table 2, column (3), but splits the sample into two subsamples. Columns (1) and (2) divide the sample according to whether a county's travel cost to the cost-minimzing domestic silver mine is above or below the median. Columns (3) and (4) divide the sample based on whether the distance of a county to the nearest domestic silver mine is above or below the median. All regressions include the full set of control variables from column (3) of Table 2. Standard errors, clustered at the prefecture level, are reported in parentheses. Significance levels: *** $p < 0.01$, ** $p < 0.05$, * $p < 0.1$.

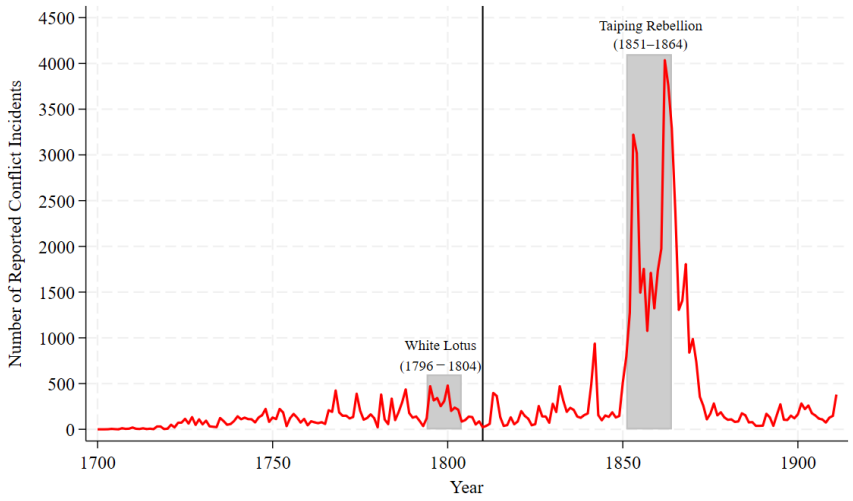

Notes: This figure plots the annual frequency of reported unrest incidents in China from 1700 to 1911. Incidents include bandit and general rule-violation activities, tax rebellions, and robberies during relief distribution, which we term conflicts, in short. The shaded periods indicate the White Lotus Rebellion (1796–1804) and the Taiping Rebellion (1851–1864). Data are from the *Qingshilu* (Veritable Records of the Qing Dynasty).

Figure B1: Conflict Frequency

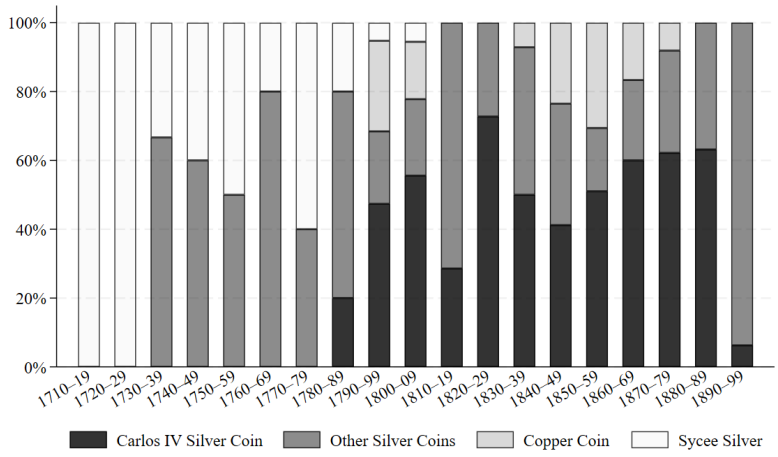

Notes: This figure is adapted Von Glahn (2007), based on data originally compiled by Yang Guozhen in *Minnan qiyue wenshu zonglu* (Comprehensive Catalogue of Contract Documents from Southern Fujian), published as a special issue of *Zhongguo Shehui Jingji Shi Yanjiu* (1990).

Figure B2: Means of Payment in Quanzhou Contracts,1710–1899

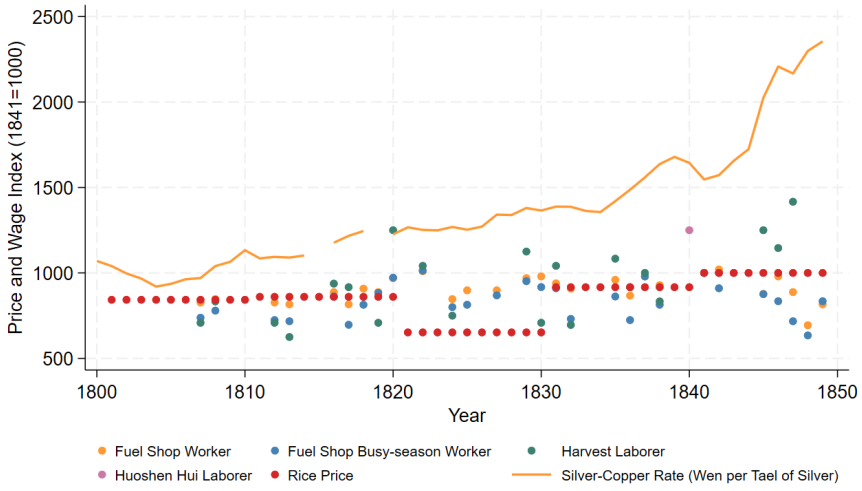

Notes: This figure plots annual wages in Beijing and national rice prices during the first half of the nineteenth century, normalized to an index of 1000 in 1841 (a year when all types have available data). Wages are recorded in copper coins and cover four types of laborers: fuel shop regular workers, fuel shop busy-season workers, harvest laborers, and Huoshen Hui laborers. Rice prices are reported in copper coins and drawn from Peng (2020). The silver–copper exchange rate as shown in Figure 3 is included here for comparison. Wage data are from Peng (2013).

Figure B3: Wages and Prices in Beijing, 1800–1850

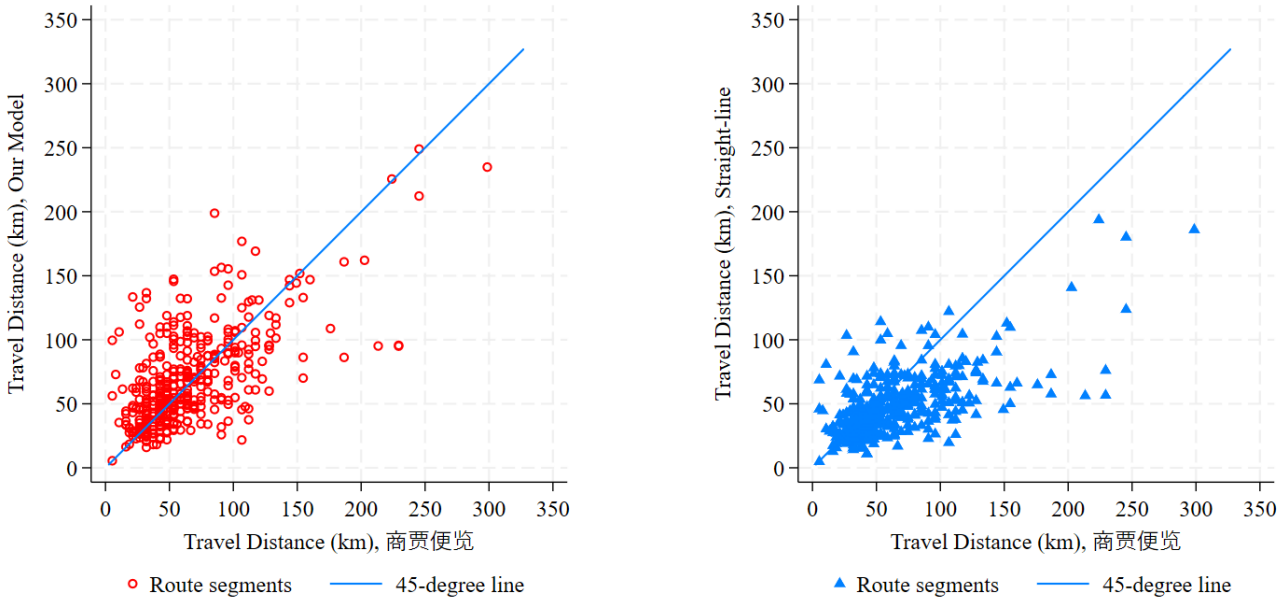

(a) Geospatial Model Estimates

(b) Straight-Line Distance

Notes: This figure validates our estimated travel distances against directly recorded travel distances from *Shangjubianlan*. Panel (a) plots estimated travel distances from our geospatial model against actual documented distances for route segments whenever such records are available. Panel (b) shows straight-line distances for comparison. Both panels include a 45-degree line for reference. The geospatial model achieves substantially better fit than straight-line distance: a simple OLS regression of documented distance on estimated distance yields a coefficient of 0.97 ($R^2 = 0.82$) for the geospatial model, compared to 0.64 for the straight-line distance.

Figure B4: Validation of Estimated Travel Distances Against Historical Records

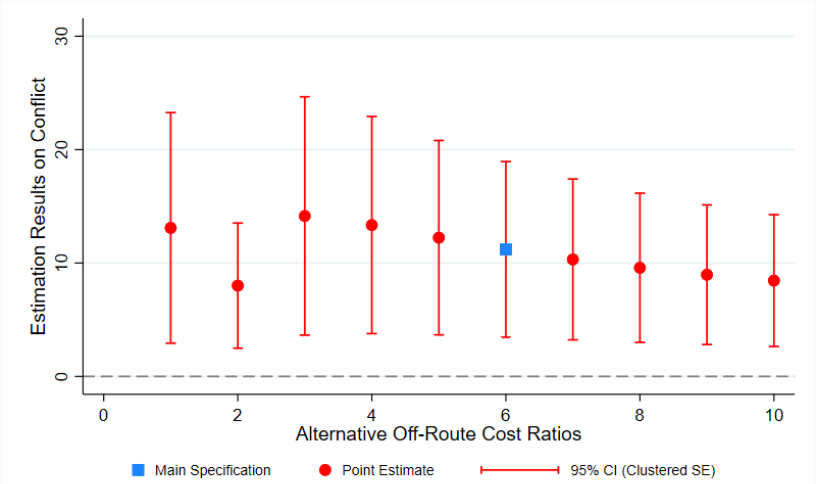

Notes: This figure reports coefficient estimates from the baseline specification (Table 2, column 4) using alternative off-route cost ratios ranging from 1 to 10 in the construction of trade costs to Canton. The blue point indicates the baseline estimate reported in the paper (off-route cost ratio = 6). Red circles represent point estimates for alternative ratios, with red vertical lines indicating 95% confidence intervals.

Figure B5: Robustness to Alternative Off-Route Cost Assumptions

C Theory Appendix

This appendix provides the proofs of the propositions stated in the paper. We maintain the assumptions from Section 4.2 that there is no domestic trade and minting.

For Propositions 2 and 3, the partial equilibrium results—abstracting from merchant profits and discussed in the main text—are straightforward to establish. Accordingly, this appendix focuses on the corresponding general equilibrium results. We further set $\lambda = 1$ and impose one regularity condition: $T - \tilde{k}\sigma < 0$, where $\tilde{k} = \frac{\sigma-1}{\sigma}k$. Let $\lambda = 1$ simplifies the analysis by removing the nonlinear dependence of imports on market size S_0. This assumption is consistent with empirical evidence, as estimates of λ are close to unity (Arkolakis, 2010; Eaton et al., 2011). The regularity condition, $T - k\sigma < 0$, implies that the tax burden cannot be too high.

Proof of proposition 1

Proof. We aim to determine the sign of $\frac{\partial^2 \ln \Delta m_i}{\partial \ln S_0 \partial \ln \tau_{i0}}$, given the functional form

$$\Delta m_i = \frac{\sigma-1}{\sigma} X_{i0} = \frac{\sigma-1}{\sigma}\left(1 - \left[\frac{S_0}{\sigma}h_i\right]^{-\lambda}\right) h_i S_0, \tag{C1}$$

where we define

$$h_i \equiv \left(\frac{\frac{\sigma}{\sigma-1}\tau_{i0}w_i/A_i}{P_0}\right)^{(1-\sigma)}.$$

Taking the natural logarithm of (C1), we obtain

$$\ln \Delta m_i = \ln\left(1 - \left[\frac{S_0}{\sigma}h_i\right]^{-\lambda}\right) + \ln h_i + \ln S_0 + \ln\frac{\sigma-1}{\sigma}.$$

Differentiating with respect to $\ln S_0$,

$$\frac{\partial \ln \Delta m_i}{\partial \ln S_0} = \frac{\lambda\left(\frac{S_0}{\sigma}h_i\right)^{-\lambda}}{1 - \left(\frac{S_0}{\sigma}h_i\right)^{-\lambda}} + 1 > 0.$$

Taking the second derivative with respect to $\ln \tau_{i0}$,

$$\frac{\partial^2 \ln \Delta m_i}{\partial \ln S_0 \partial \ln \tau_{i0}} = -\frac{\lambda^2 S_0}{\sigma} \frac{\left(\frac{S_0}{\sigma} h_i\right)^{-(\lambda+1)}}{(1-\left(\frac{S_0}{\sigma} h_i\right)^{-\lambda})^2} \cdot \frac{\partial h_i}{\partial \ln \tau_{i0}}.$$

Since $-\frac{\lambda^2 S_0}{\sigma}$ is negative, the factor $\frac{\left(\frac{S_0}{\sigma} h_i\right)^{-(\lambda+1)}}{(1-\left(\frac{S_0}{\sigma} h_i\right)^{-\lambda})^2}$ is strictly positive, the sign of $\frac{\partial^2 \ln \Delta m_i}{\partial \ln S_0 \partial \ln \tau_{i0}}$ depends on the sign of $\frac{\partial h_i}{\partial \ln \tau_{i0}}$. Given that $\sigma > 1$, we have $\frac{\partial h_i}{\partial \ln \tau_{i0}} < 0$. Thus,

$$\frac{\partial^2 \ln \Delta m_i}{\partial \ln S_0 \partial \ln \tau_{i0}} > 0.$$

□

Proof of Proposition 2 (GE case)

Proof. For expositional simplicity, we suppress the subscript i when possible. Absent domestic trade and minting, using Equation (15) to substitute Δm in Equation (8), the latter can be written as an implicit function:

$$G(w, S_0, \tau, T) = wL - T - \tilde{k}\left(1 - \left[\frac{S_0}{\sigma} h\right]^{-\lambda}\right) h S_0 = 0. \tag{C2}$$

With $\lambda = 1$, we can show that the partial derivatives of G with respect to S_0, w, τ, and T are given by:

$$\frac{\partial G}{\partial S_0} = -\tilde{k}h \qquad \frac{\partial G}{\partial w} = L + \tilde{k} S_0 (\sigma - 1)\frac{h}{w} \qquad \frac{\partial G}{\partial \tau} = \tilde{k} S_0 (\sigma - 1)\frac{h}{\tau} \qquad \frac{\partial G}{\partial T} = -1 \tag{C3}$$

First-order derivative $\frac{d \ln w}{d \ln S_0}$. Using implicit differentiation on the equilibrium condition:

$$\frac{d \ln w}{d \ln S_0} = -\frac{S_0}{w} \cdot \frac{\frac{\partial G}{\partial S_0}}{\frac{\partial G}{\partial w}} = \frac{S_0 \tilde{k} h}{wL + \tilde{k} S_0 (\sigma - 1) h} > 0 \tag{C4}$$

Without domestic trade, regions consume only the locally produced variety, making the silver-denominated local price index proportional to local wages. Consequently, a decline in foreign

silver supply (lower S_0) generates silver appreciation, as goods and labor become cheaper in silver terms (lower w_i).

Second-order cross derivative $\frac{d^2 \ln w}{d \ln S_0 \, d \ln \tau}$. Knowing that $G(w, S_0, \tau, T) = 0$, we have $wL = T + \tilde{k}\left(1 - \left[\frac{S_0}{\sigma}h\right]^{-1}\right) hS_0$. Substituting for wL, the elasticity of wage with respect to S_0 becomes

$$\frac{d \ln w}{d \ln S_0} = \frac{S_0 \tilde{k} h}{T + \tilde{k} h S_0 \left(\sigma - \left[\frac{S_0}{\sigma}h\right]^{-1}\right)} > 0. \tag{C5}$$

The cross derivative is then given by:

$$\frac{d^2 \ln w}{d \ln S_0 d \ln \tau} = \frac{\tau S_0 \tilde{k}(T - \tilde{k}\sigma)}{\left[T + \tilde{k}\sigma(hS_0 - 1)\right]^2} \frac{dh}{d\tau} \tag{C6}$$

To evaluate this expression, we need $\frac{dh}{d\tau}$. Since $h = \left(\frac{\sigma}{\sigma - 1}\frac{\tau w}{AP_0}\right)^{(1-\sigma)}$, we have:

$$\frac{dh}{d\tau} = (1 - \sigma) h \left[\frac{1}{\tau} + \frac{1}{w}\frac{dw}{d\tau}\right] \tag{C7}$$

Using the implicit function theorem, we obtain:

$$\frac{dw}{d\tau} = -\frac{\frac{\partial G}{\partial \tau}}{\frac{\partial G}{\partial w}} = -\frac{\tilde{k} S_0 (\sigma - 1)\frac{h}{\tau}}{L + \tilde{k} S_0 (\sigma - 1)\frac{h}{w}} < 0 \tag{C8}$$

Substituting this result back to $\frac{dh}{d\tau}$, we get:

$$\frac{dh}{d\tau} = (1 - \sigma) h \frac{1}{\tau}\left[1 - \frac{\tilde{k} S_0 (\sigma - 1)}{\frac{wL}{h} + \tilde{k} S_0 (\sigma - 1)}\right] < 0 \tag{C9}$$

Finally, combining these results:

$$\frac{d^2 \ln w}{d \ln S_0 d \ln \tau} = \frac{\tau S_0 \tilde{k}(T - \tilde{k}\sigma)}{\left[T + \tilde{k}\sigma(hS_0 - 1)\right]^2} \frac{dh}{d\tau} \tag{C10}$$

With the regularity condition $T - \tilde{k}\sigma < 0$ and $\frac{dh}{d\tau} < 0$, we have:

$$\frac{d^2 \ln w}{d \ln S_0 d \ln \tau} > 0 \tag{C11}$$

This positive cross derivative implies that the wage or local price elasticity with respect to foreign market size increases with trade costs. Consequently, when the foreign silver supply declines, the resulting decrease in goods prices is more pronounced in regions that are farther from the international trade hub—that is, these areas experience *greater silver appreciation*. □

Proof of Proposition 3 (GE case)

Proof. From equation (16), we know that the equilibrium one-period utility (welfare) of an individual is given by:

$$\ln \omega = C_0 + (1+\gamma) \ln \left(\frac{\Delta m}{k \Delta m + T} \right),$$

where C_0 is a constant. Using equation (C1) and $\lambda = 1$ to substitute Δm, we get:

$$\ln \omega = \underbrace{C_0 + \ln \frac{\sigma - 1}{\sigma}}_{Constant} + (1+\gamma) \ln(hS_0 - \sigma) - (1+\gamma) \ln(\tilde{k} h S_0 - \tilde{k}\sigma + T). \tag{C12}$$

First-order derivative $\frac{d \ln \omega}{d \ln S_0}$. Applying the chain rule, we have:

$$\frac{d \ln \omega}{d \ln S_0} = (1+\gamma) S_0 h \left(\frac{d \ln h}{d \ln S_0} + 1 \right) \left[\frac{1}{hS_0 - \sigma} - \frac{\tilde{k}}{\tilde{k} h S_0 - \tilde{k}\sigma + T} \right] \tag{C13}$$

Where

$$\frac{d \ln h}{d \ln S_0} + 1 = (1-\sigma) \frac{d \ln w}{d \ln S_0} + 1 = \frac{\tilde{k} h S_0 + T - \tilde{k}\sigma}{T + \tilde{k}\sigma(hS_0 - 1)}.$$

Therefore,

$$\frac{d \ln \omega}{d \ln S_0} = (1+\gamma) \frac{S_0 h T}{(hS_0 - \sigma)[T + \tilde{k}\sigma(hS_0 - 1)]} > 0. \tag{C14}$$

The inequality is guaranteed by condition (C5), which implies $T + \tilde{k}\sigma(hS_0 - 1) > 0$, and by the fact that $f \leq 1$ (f is the share of buyers reached), which in turn implies $hS_0 > \sigma$. That is, when aggregate silver inflows decrease, regional welfare decreases.

Second-order cross derivative $\frac{d^2 \ln \omega}{d \ln S_0 \, d \ln \tau}$. Applying the chain rule:

$$\frac{d^2 \ln \omega}{d \ln S_0 \, d \ln \tau} = (1+\gamma) \frac{S_0 T \sigma \tilde{k} [\sigma - \frac{T}{\tilde{k}} - h^2 S_0^2]}{[(hS_0 - \sigma)[T + \tilde{k}\sigma(hS_0 - 1)]]^2} \frac{dh}{d \ln \tau} \tag{C15}$$

With the expression for $\frac{dh}{d\tau}$ derived earlier, the equation above becomes:

$$\frac{d^2 \ln \omega}{d \ln S_0 d \ln \tau} = (1+\gamma)(\sigma - 1) \frac{S_0 T \sigma h (\tilde{k} h^2 S_0^2 + T - \tilde{k}\sigma)}{[(hS_0 - \sigma)[T + \tilde{k}\sigma(hS_0 - 1)]]^2} \left[1 - \frac{\tilde{k} S_0 (\sigma - 1)}{\frac{wL}{h} + \tilde{k} S_0 (\sigma - 1)} \right]. \tag{C16}$$

Except for the term $\tilde{k} h^2 S_0^2 + T - \tilde{k}\sigma$, the remaining terms are clearly positive. The inequality $hS_0 > \sigma$ implies

$$\tilde{k} h^2 S_0^2 + T - \tilde{k}\sigma > \tilde{k} h S_0 \sigma + T - \tilde{k}\sigma,$$

and we have previously established that the right-hand side is positive. It follows that the term $\tilde{k} h^2 S_0^2 + T - \tilde{k}\sigma$ is also positive. Therefore,

$$\frac{d^2 \ln \omega}{d \ln S_0 \, d \ln \tau} > 0.$$

How does T affect the value of $\frac{d^2 \ln \omega}{d \ln S_0 \, d \ln \tau}$. We are interested in how $\frac{d^2 \ln \omega}{d \ln S_0 \, d \ln \tau}$ changes with respect to T. To simplify the expression, we define $F = \frac{1}{C_1} \frac{d^2 \ln \omega}{d \ln S_0 \, d \ln \tau}$ where $C_1 = \frac{1}{(1+\gamma)(\sigma-1) S_0 \sigma}$ and is a constant. We then compute $\frac{dF}{dT}$; if this derivative is positive, it follows that $\frac{d}{dT} \left(\frac{d^2 \ln \omega}{d \ln S_0 \, d \ln \tau} \right)$ is also positive. After this simplification, we have

$$F = \underbrace{\frac{T h (\tilde{k} h^2 S_0^2 + T - \tilde{k}\sigma)}{[(hS_0 - \sigma)(T + \tilde{k}\sigma(hS_0 - 1))]^2}}_{F_1} \underbrace{\left[1 - \frac{\tilde{k} S_0 (\sigma - 1)}{\frac{wL}{h} + \tilde{k} S_0 (\sigma - 1)} \right]}_{F_2} \tag{C17}$$

Therefore, its total derivative with respect to T is given by

$$\frac{dF}{dT} = \frac{\partial F_1}{\partial T} \cdot F_2 + \frac{\partial F_1}{\partial h} \frac{dh}{dT} \cdot F_2 + F_1 \cdot \frac{\partial F_2}{\partial (w/h)} \cdot \frac{d(w/h)}{dT} \tag{C18}$$

We have previously shown that both F_1 and F_2 are positive. It is also straightforward to verify that F_2 increases with w/h, i.e., $\frac{\partial F_2}{\partial (w/h)} > 0$. Therefore, to prove $\frac{dF}{dT} > 0$, it is sufficient to compute

the signs of the following derivatives

$$\frac{\partial F_1}{\partial T}, \quad \frac{\partial F_1}{\partial h} \cdot \frac{dh}{dT}, \quad \text{and} \quad \frac{d(w/h)}{dT},$$

and show that they are all positive. We proceed by analyzing them one at a time.

Step 1. First, we compute $\frac{\partial F_1}{\partial T}$:

$$\begin{aligned}\frac{\partial F_1}{\partial T} &= \frac{h(\tilde{k}h^2S_0^2 + T - \tilde{k}\sigma)(T + \tilde{k}\sigma(hS_0 - 1)) + Th(T + \tilde{k}\sigma(hS_0 - 1)) - 2Th(\tilde{k}h^2S_0^2 + T - \tilde{k}\sigma)}{(hS_0 - \sigma)^2(T + \tilde{k}\sigma(hS_0 - 1))^3} \\ &= \frac{h[(\tilde{k}h^2S_0^2 + 2T - \tilde{k}\sigma)(T + \tilde{k}\sigma(hS_0 - 1)) - 2T(\tilde{k}h^2S_0^2 + T - \tilde{k}\sigma)]}{(hS_0 - \sigma)^2(T + \tilde{k}\sigma(hS_0 - 1))^3}.\end{aligned}$$

To establish the sign, we analyze the numerator. Dividing by $h > 0$, we need to show:

$$\underbrace{(\tilde{k}h^2S_0^2 + 2T - \tilde{k}\sigma)(T + \tilde{k}\sigma(hS_0 - 1)) - 2T(\tilde{k}h^2S_0^2 + T - \tilde{k}\sigma)}_{F_3} > 0$$

Denote the left-hand side of the expression as F_3. Expanding and collecting terms, we obtain:

$$F_3 = T\tilde{k}[-h^2S_0^2 + \sigma(2hS_0 - 1)] + \tilde{k}^2\sigma(hS_0 - 1)(h^2S_0^2 - \sigma)$$

Since $hS_0 > \sigma > 1$, we have $(hS_0 - 1) > 0$ and $(h^2S_0^2 - \sigma) > 0$. Given $\tilde{k}\sigma > T$, we establish that:

$$\tilde{k}^2\sigma(hS_0 - 1)(h^2S_0^2 - \sigma) > T\tilde{k}(hS_0 - 1)(h^2S_0^2 - \sigma)$$

Therefore, the expression exceeds:

$$\begin{aligned}F_3 &> T\tilde{k}[-h^2S_0^2 + \sigma(2hS_0 - 1)] + T\tilde{k}(hS_0 - 1)(h^2S_0^2 - \sigma) \\ &= T\tilde{k}[(hS_0 - 1)(h^2S_0^2 - \sigma) - h^2S_0^2 + \sigma(2hS_0 - 1)]\end{aligned}$$

Simplifying the bracketed term on the right-hand side:

$$(hS_0 - 1)(h^2S_0^2 - \sigma) - h^2S_0^2 + \sigma(2hS_0 - 1) = hS_0(h^2S_0^2 + \sigma - 2hS_0)$$

Note that $h^2S_0^2 + \sigma - 2hS_0 = (hS_0 - 1)^2 + (\sigma - 1)$. Since $\sigma > 1$, we have $(hS_0 - 1)^2 + (\sigma - 1) > 0$. Thus, $\frac{\partial F_1}{\partial T} > \frac{hT\tilde{k}hS_0[(hS_0-1)^2+(\sigma-1)]}{(hS_0-\sigma)^2(T+\tilde{k}\sigma(hS_0-1))^3} > 0$, completing the proof that $\frac{\partial F_1}{\partial T}$ is positive.

Step 2. Second, we compute $\frac{\partial F_1}{\partial h}$:

$$\frac{\partial F_1}{\partial h} = \frac{T(\tilde{k}h^2S_0^2 + T - \tilde{k}\sigma)}{[(hS_0 - \sigma)(T + \tilde{k}\sigma(hS_0 - 1))]^2} \underbrace{\left[1 + \frac{2\tilde{k}h^2S_0^2}{\tilde{k}h^2S_0^2 + T - \tilde{k}\sigma} - \frac{2hS_0}{hS_0 - \sigma} - \frac{2h\tilde{k}\sigma S_0}{T + \tilde{k}\sigma(hS_0 - 1)}\right]}_{F_4}.$$

The first fraction in the above expression is positive. Denote the second term as F_4; it equals:

$$F_4 = \frac{2\tilde{k}hS_0(S_0 - \sigma)(T - \tilde{k}\sigma) - (hS_0 + \sigma)[\tilde{k}h^2S_0^2 + T - \tilde{k}\sigma][T + \tilde{k}\sigma(hS_0 - 1)]}{[\tilde{k}h^2S_0^2 + T - \tilde{k}\sigma][T + \tilde{k}\sigma(hS_0 - 1)][hS_0 - \sigma]}. \tag{C19}$$

In equation (C19), all three bracketed terms in the denominator are positive. In the numerator, the second term (after the minus sign) is positive. Moreover, by the regularity condition $T < \tilde{k}\sigma$, the first term in the numerator, $2\tilde{k}hS_0(S_0 - \sigma)(T - \tilde{k}\sigma)$, is negative.[29] Therefore, the whole term is negative, which implies that $\frac{\partial F_1}{\partial h} < 0$.

Step 3. Finally, recall that in the proof of Proposition 2, we computed:

$$\frac{\partial G}{\partial w} = L - \tilde{k}S_0(1 - \sigma)\frac{h}{w}, \qquad \frac{\partial G}{\partial T} = -1,$$

It follows that

$$\frac{dw}{dT} = -\frac{\frac{\partial G}{\partial T}}{\frac{\partial G}{\partial w}} > 0, \quad \text{and hence} \quad \frac{dh}{dT} = (1 - \sigma)\frac{h}{w}\frac{dw}{dT} < 0.$$

And

$$\frac{d(w/h)}{dT} = \frac{1}{h}\frac{dw}{dT} - \frac{w}{h^2}\frac{dh}{dT} = \frac{\sigma}{h}\frac{dw}{dT} > 0.$$

Therefore, $\frac{\partial F_1}{\partial h} \times \frac{dh}{dT}$ is positive and $\frac{d(w/h)}{dT}$ is also positive. Combined with what we proved in Step 1, it follows that all three terms – $\frac{\partial F_1}{\partial T}$, $\frac{\partial F_1}{\partial h} \times \frac{dh}{dT}$, and $\frac{d(w/h)}{dT}$ – are positive. Hence, $\frac{dF}{dT}$ is positive, and the proof is complete. □

To summarize, the greater the silver-denominated tax T, the greater the value of $\frac{d^2 \ln \omega}{d \ln S_0 \, d \ln \tau}$. Combined with the fact that $\frac{d^2 \ln \omega}{d \ln S_0 \, d \ln \tau} > 0$, as we proved earlier, this implies that when aggregate

[29] Although we did not prove this explicitly, $S_0 - \sigma > 0$ clearly holds, since $hS_0 > \sigma$ and $h \leq 1$.

foreign silver supply declines, regions with higher trade costs to Canton experience greater welfare declines and, consequently, higher conflict incidence. This effect is more pronounced when the local tax burden is high.

Appendix References

ARKOLAKIS, C. (2010): "Market Penetration Costs and the New Consumers Margin in International Trade," *Journal of Political Economy*, 118, 1151–1199.

BAI, Y., X. BIAN, AND R. JIA (2025): "Endogenous Canal: How Did National Capital Relocation Reshape Economic Geography in Historical China?" Unpublished manuscript.

BORAH, W. W. (1949): "The Mining Guild of New Spain and Its Tribunal General 1770-1821," .

CAO, S. (2001): *Zhongguo renkoushi (Qing shiqi) (The Population History of China (Qing Dynasty))*, Shanghai: Fudan University Press, (in Chinese).

CAO, Y. AND S. CHEN (2022): "Rebel on the Canal: Disrupted Trade Access and Social Conflict in China, 1650–1911," *American Economic Review*, 112, 1555–1590.

CHGIS (2016a): "1820 Layers GBK Encoding," Dataset.

——— (2016b): "China Historical GIS Version 6," Cambridge, MA and Shanghai.

DAI, Y. (2019): *The White Lotus War: Rebellion and Suppression in Late Imperial China*, University of Washington Press.

EAST ASIA RESEARCH INSTITUTE (1943): *Basic Agricultural Statistical Data of China: "Agricultural Reports" (1931-1936) - Mengjiang and Chinese Provinces. Multi-year Statistical Compilation. Volume 2*, Compilation of Research on East Asian Food Issues, East Asia Research Institute.

EATON, J., S. KORTUM, AND F. KRAMARZ (2011): "An Anatomy of International Trade: Evidence from French Firms," *Econometrica*, 79, 1453–1498.

EUROPEAN SPACE AGENCY (2022): "Copernicus DEM," Digital Elevation Model Dataset.

FEARON, J. D. AND D. D. LAITIN (2003): "Ethnicity, Insurgency, and Civil War," *American Political Science Review*, 97, 75–90.

FLYNN, D. O. AND A. GIRÁLDEZ (2022): "Born with a 'Silver Spoon': The Origin of World Trade in 1571," in *Metals and Monies in an Emerging Global Economy*, Routledge, 259–279.

FOOD AND AGRICULTURE ORGANIZATION OF THE UNITED NATIONS (FAO) AND INTERNATIONAL INSTITUTE FOR APPLIED SYSTEMS ANALYSIS (IIASA) (2021): "Global Agro-Ecological Zones (GAEZ) Model Version 4," `https://gaez.fao.org`.

GALOR, O. AND Ö. ÖZAK (2016): "The Agricultural Origins of Time Preference," *American Economic Review*, 106, 3064–3103.

GUO, Y. (2022): *Land and Labor Tax in Imperial Qing China (1644-1912)*, vol. 18, Brill.

HE, P. (2008): *Qingdai fuishui zhengce yanjiu (Studies on Qing Dynasty Taxation Policy)*, Beijing: China Social Sciences Press, (in Chinese).

HU, Y. (2021): "Qingdai yinqian bijia bodong yanjiu (1644–1911) (Research on the Exchange Rate Fluctuation between Silver and Copper Coin in the Qing Dynasty (1644–1911))," Ph.D. thesis, East China Normal University, Shanghai, (in Chinese).

KUHN, P. A. (1990): *Soulstealers: The Chinese Sorcery Scare of 1768*, Cambridge, MA: Harvard University Press.

——— (2002): *Rebellion and Its Enemies in Late Imperial China: Militarization and Social Structure, 1796-1864*, Cambridge, MA: Harvard University Press.

LEE, L. (2009): "Estimating the Yearly Amount of Silver Inflow during the Ching Dynasty in China (1645-1911)," *Journal of Humanities and Social Sciences*, 5, 31–58.

LIN, M.-H. (2020): "China Upside Down: Currency, Society, and Ideologies, 1808–1856," in *China Upside Down*, Harvard University Asia Center.

LIU, C.-Y. (1993): ""Chong, Fan, Pi, Nan": Qingdai Dao, Fu, Ting, Zhou, Xian dengji chutan ("Cong, Fan, Pi, Nan": A Preliminary Study of the Hierarchy of Circuits, Prefectures, Departments, Subprefectures, and Counties in the Qing Dynasty)," *Bulletin of the Institute of History and Philology, Academia Sinica*, 64, 175–204, (in Chinese).

NI, S. AND P. H. VAN (2006): "High Corruption Income in Ming and Qing China," *Journal of Development Economics*, 81, 316–336.

NOAA (1999): "Global Land One-km Base Elevation (GLOBE) Project," Version 1.0. Accessed: 2025-07-20.

PENG, K. (2013): "Jindai Beijing jiage yu gongzi de bianqian: 19 shiji chu zhi 20 shiji chu (Changes in Prices and Wages in Modern Beijing: From the Early Nineteenth Century to the Early Twentieth Century)," *Journal of Hebei University (Philosophy and Social Science Edition)*, (in Chinese).

PENG, X. (2020): *Zhongguo huobi shi (A Monetary History of China)*, Shanghai: Shanghai People's Publishing House, 4th ed., (in Chinese, originally published in 1958).

RICHARDS, J. F. (2002): "The Opium Industry in British India," *The Indian Economic & Social History Review*, 39, 149–180.

SCHEIDEL, W. AND E. MEEKS (2012): "ORBIS: The Stanford Geospatial Network Model of the Roman World," `http://orbis.stanford.edu`, version 2.0.

SHI, Z. (2009): *Qingdai hubu: yinku shouzhi he kucun tongji (Statistics on Revenue, Expenditure, and Inventory of the Ministry of Revenue Vault in the Qing Dynasty)*, Fuzhou: Fujian People's Publishing House, (in Chinese).

SNG, T.-H. (2014): "Size and Dynastic Decline: The Principal-Agent Problem in Late Imperial China, 1700–1850," *Explorations in Economic History*, 54, 107–127.

VILAR, P. (1991): *A History of Gold and Money, 1450-1920*, New York: Verso.

WANG, H. (2008): *Zhongguo jiapu zongmu (Comprehensive Catalogue of Chinese Genealogies)*, Shanghai: Shanghai Ancient Books Publishing House, (in Chinese).

WEI, Q. (1983): *Qingdai de kuangye (Mining in the Qing Dynasty. Volume 2)*, Beijing: Zhonghua Book Company, (in Chinese).

ZHANG, D. (2013): *Zhongguo sanqiannian qixiang jiluzongji (A Comprehensive Collection of Meteorological Records of China over the Past 3000 Years)*, Nanjing: Jiangsu Education Press, (in Chinese).